FINAL TECHNICAL REPORT

Submitted To

Dr. LARRY KABACOFF
OFFICE OF NAVAL RESEARCH
CODE 1131
800 NORTH QUINCY STREET
ARLINGTON, VA 22217 - 5000

For The Period

AUGUST 15, 1992 - AUGUST 14, 1995

MODELING THE DAMPING BEHAVIOR OF COMPOSITES USING FEM

By

S. ANKEM, K. S. KANNAN, A. NANAVATY, J. G. RAO AND S. A . SRINIVASAN

ONR N00014-92-J-4039

JUNE 1996

REPORT DOCUMENTATION PAGE

Form Approved
OMB No. 0704-0188

1. AGENCY USE ONLY (Leave blank)	2. REPORT DATE	3. REPORT TYPE AND DATES COVERED
	June 1996	August 15, 1992-August 14, 1995

4. TITLE AND SUBTITLE
Modeling the Damping Behavior of Composites Using FEM

5. FUNDING NUMBERS

6. AUTHOR(S)
S. Ankem, K. S. Kannan, A. Nanavaty, J. G. Rao and S. A. Srinivasan

7. PERFORMING ORGANIZATION NAME(S) AND ADDRESS(ES)
University of Maryland
Dept. of Materials and Nuclear Engineering
College Park, MD 20742-2115

8. PERFORMING ORGANIZATION REPORT NUMBER
ONR

9. SPONSORING / MONITORING AGENCY NAME(S) AND ADDRESS(ES)
Office of Naval Research
Code 1131
800 North Quincy Street
Arlington, VA 22217-5000

10. SPONSORING / MONITORING AGENCY REPORT NUMBER
N00014-92-J-4039

11. SUPPLEMENTARY NOTES

12a. DISTRIBUTION / AVAILABILITY STATEMENT
Unlimited

12b. DISTRIBUTION CODE

13. ABSTRACT (Maximum 200 words)

The damping behavior of Aluminum-Epoxy composites has been successfully predicted by using the finite element method. It was shown that the loss factor of a given composite depends on morphology and volume percent of component phases. For a given volume percent of Aluminum or Epoxy, the loss factor is found to increase with an increase in relative particle size. This was attributed to the ability of the high damping epoxy phase to damp/deform relatively freely when the particle size was increased. A 3-D plot with loss factor, relative particle size, and volume percent of Aluminum as the parameters was constructed which clearly demonstrates the effect of particle size and volume percent of phases on the damping behavior of epoxy/aluminum composites.

14. SUBJECT TERMS			15. NUMBER OF PAGES: 36
			16. PRICE CODE
17. SECURITY CLASSIFICATION OF REPORT	18. SECURITY CLASSIFICATION OF THIS PAGE	19. SECURITY CLASSIFICATION OF ABSTRACT	20. LIMITATION OF ABSTRACT

DISCLAIMER NOTICE

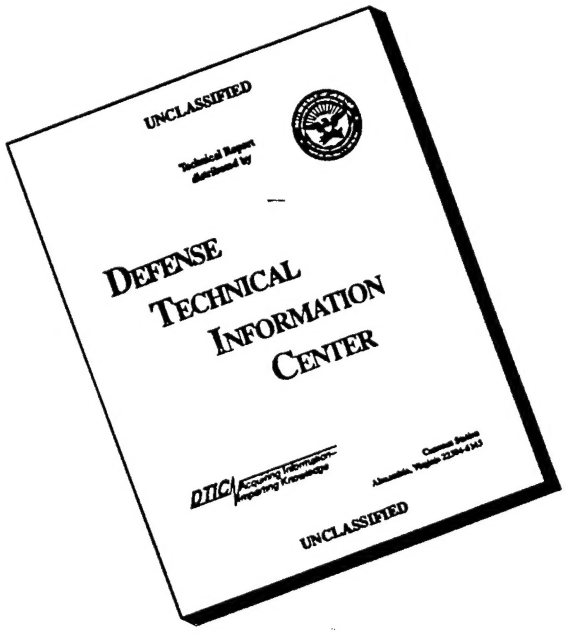

THIS DOCUMENT IS BEST QUALITY AVAILABLE. THE COPY FURNISHED TO DTIC CONTAINED A SIGNIFICANT NUMBER OF PAGES WHICH DO NOT REPRODUCE LEGIBLY.

REPORT DOCUMENTATION PAGE

Form Approved
OMB No. 0704 0188

1. AGENCY USE ONLY (Leave blank)	2. REPORT DATE	3. REPORT TYPE AND DATES COVERED
	June 1996	August 15, 1992–August 14, 1995

4. TITLE AND SUBTITLE
Modeling the Damping Behavior of Composites Using FEM

5. FUNDING NUMBERS

6. AUTHOR(S)
S. Ankem, K. S. Kannan, A. Nanavaty, J. G. Rao and
S. A. Srinivasan

7. PERFORMING ORGANIZATION NAME(S) AND ADDRESS(ES)
University of Maryland
Dept. of Materials and Nuclear Engineering
College Park, MD 20742-2115

8. PERFORMING ORGANIZATION REPORT NUMBER
ONR

9. SPONSORING/MONITORING AGENCY NAME(S) AND ADDRESS(ES)
Office of Naval Research
Code 1131
800 North Quincy Street
Arlington, VA 22217-5000

10. SPONSORING/MONITORING AGENCY REPORT NUMBER
N00014-92-J-4039

11. SUPPLEMENTARY NOTES

12a. DISTRIBUTION/AVAILABILITY STATEMENT

12b. DISTRIBUTION CODE

13. ABSTRACT (Maximum 200 words)

The damping behavior of Aluminum-Epoxy composites has been successfully predicted by using the finite element method. It was shown that the loss factor of a given composite depends on morphology and volume percent of component phases. For a given volume percent of Aluminum or Epoxy, the loss factor is found to increase with an increase in relative particle size. This was attributed to the ability of the high damping epoxy phase to damp/deform relatively freely when the particle size was increased. A 3-D plot with loss factor, relative particle size, and volume percent of Aluminum as the parameters was constructed which clearly demonstrates the effect of particle size and volume percent of phases on the damping behavior of epoxy/aluminum composites.

14. SUBJECT TERMS			15. NUMBER OF PAGES 36
			16. PRICE CODE
17. SECURITY CLASSIFICATION OF REPORT	18. SECURITY CLASSIFICATION OF THIS PAGE	19. SECURITY CLASSIFICATION OF ABSTRACT	20. LIMITATION OF ABSTRACT

Table of Contents

1. Project Summary 1

2A. Technical Progress : Part I 3

2B. Technical Progress : Part II 15

2C. Technical Progress : Part III 20

3. Technical Presentations and Publications 29

4. Appendix : Sample Input and Output for a 50 Volume

Percent Aluminium-Epoxy Composite 30

1. PROJECT SUMMARY

The aim of this program was to systematically study the effect of volume percent and morphology of phases on the damping behavior of epoxy/aluminium composites. This has been successfully achieved by employing the finite element method (FEM) to predict the effect of volume fraction, morphology (including particle shape, size and orientation), and continuity of phases on the damping behavior using the ANSYS or NASTRAN computer programs. The technical progress during this investigation is divided into three parts and each part is self-contained in all respects. A sample input and output is also provided as an appendix in the end for an FEM calculation involving 50 volume percent of aluminium/ 50 volume percent of epoxy composite. This calculation was performed with the ANSYS computer program.

Part I is a comprehensive review of the recent developments in modeling the damping behavior of composites in general. In this review it was concluded that in general analytical methods can be employed only to relatively simple geometries and composite configurations. Even for the simple cases, analytical methods developed are usually specific to geometry and configuration. Numerical methods like FEM, however, have the potential for application to arbitrary composite geometry and configuration and arbitrary loading conditions. The review includes analytical models for both passive and active damping.

In Part II a brief account of the effect of morphology and volume fraction on the damping behavior of epoxy/aluminium composites is given. This also includes the author's earlier work. In this part it has been clearly shown that for a given volume percent of phases the damping capacity of the composites strongly depend on particle size of the component phases. It has been found that the loss factors do not decrease linearly with the volume percent of the second phase. For particulate composites, the loss factors are much lower than what is expected from the law of mixtures. The actual size was found to depend on the particle size of the phases.

The results of extensive FEM modeling to predict the effect of volume percent and morphology of phases on the damping behavior of epoxy/aluminium composites have been presented in Part III. It was shown that the loss factor of the composites with parallel and perpendicular fibers calculated by FEM were close to those obtained by analytical methods based on the constant strain and constant stress assumptions. For a given volume percent of aluminium or epoxy, the loss factor was found to increase with an increase in relative particle size. This was attributed to the ability of the high damping epoxy to damp/deform relatively freely when the particle size was increased. A 3-D plot with loss factor, relative particle size, and volume percent of aluminium as the parameters was constructed for the epoxy/aluminium composites, which clearly demonstrates the effect of particle size and volume percent of phases on the damping behavior. For a composite with 50 volume percent of each phase, the loss factor of the composite, when the Aluminium phase was embedded as a single particle in the epoxy matrix, was found to be much higher than when the particles were reversed. This has been attributed to the ability of the epoxy to damp/deform relatively independently when it is in the matrix phase. For various epoxy/aluminium composites, normal stress distributions were also studied. They show that in general the stresses are higher in the stiffer aluminium phase whether aluminium is in the form of particles or matrix. The extent of stress gradients depend on the volume fraction and particle size.

Two dimensional hydrostatic stress distributions were also calculated for various epoxy/aluminium composites. It was found that the magnitude of stress gradients increased with an increase in particle size for a given volume percent of phases. These results have suggested that the propensity for void or crack formation increased with an increase in particle size.

2A. TECHNICAL PROGRESS : PART I

Proceedings of the Damping of Multiphase Inorganic Materials Symposium, ASM Materials Week, Chicago, Illinois, USA, 2-5 November 1992

Recent Developments in Modeling the Damping Behaviour of Composites

K.S. Kannan and S. Ankem
University of Maryland
College Park, Maryland

Abstract

Many investigators have attempted to model the damping behaviour of composite materials using different analytical and numerical techniques including FEM. The extensive review indicates that the analytical techniques are primarily suitable for specific and idealized composite structures, whereas FEM can be applied to the modeling of even complicated structures. This method can effectively take a number of factors such as morphology (i.e., size, shape and distribution of phases), volume fraction and properties of the component phases into consideration simultaneously. The viability of this method is illustrated with the recent work of the authors and of other investigators. In addition, the recent developments relating to the modeling of the active damping of composites structures using embedded, distributed sensors and actuators are presented.

MULTIPHASE materials such as composites are used in several applications involving dynamic loading conditions. To reduce noise or unwanted vibrations, damping of the structure needs to be improved. This may be done in several ways - passively by enhancing damping of a structure by using materials with better internal damping and / or by optimizing the internal structural configuration , and / or actively by including actuators which oppose and suppress undesired vibrations. To design new composite materials with high damping properties or to improve the damping of the existing materials, it is necessary to understand the damping behaviour in terms of the damping properties of the component phases and their volume fractions and morphologies. The aim of this paper is to review the models available for predicting the passive as well as active damping of composite materials and structures.

Modeling of Passive Damping

To model or predict the dynamic response of a composite structure, it is essential to consider the damping properties, volume fraction , morphology and the nature of the interfaces between the component phases. Most of the analytical solutions available to date take into account only some of these factors and they are confined to specific and simple geometries. However, some of the numerical methods such as the finite element method can take most of these factors simultaneously into consideration. The analytical and numerical methods are dealt with in separate sections.

.Analytical Methods. Viscoelastic behaviour of a material is characterised by a response (displacement / strain in the appropriate deformation mode) that lags behind applied force / stress. A composite would exhibit viscoelastic behaviour even if one of the component phases is viscoelastic. Viscoelastic material behaviour in a particular deformation mode is frequently represented through frequency dependent complex moduli - extensional, shear, bulk - and / or poisson's ratio. For example, the Youngs modulus is represented in complex form as :

$$\tilde{E} = E_0(1 + i\eta) = E_0 + iE_1 \qquad \ldots\ldots 1$$

$\tilde{E}$ is complex modulus, E_0 is the storage modulus representing strain energy, E_1 ($= E_0\eta$) is the loss modulus representing energy dissipated and η is the loss factor (1). This representation is obtained from a hereditary integral type representation of the constitutive relationship in a viscoelastic material (2) :

$$\sigma_{ij} = \int_{-t}^{\infty} C_{ijkl}(t-\tau)(d\varepsilon_{kl}/dt)d\tau \quad \text{..... 2}$$

where $C_{ijkl}(t-\tau)$ are the relaxation constants, t is time, σ_{ij} is the stress tensor and ε_{kl} is the strain tensor. For a one dimensional state of stress, this reduces to

$$\sigma_1(t) = \int_{-t}^{\infty} E'(t-\tau)(d\varepsilon_1/dt)d\tau \quad \text{..... 3}$$

where $\tilde{E}$, the frequency dependent complex modulus, eq. 1, is related to E' through the inverse Fourier transform

$$E'(t) = F^{-1}[\tilde{E}(\omega)/(i\omega)] \quad \text{.... 4}$$

The most frequently encountered analytical method for prediction of damping behaviour of composite structures uses micromechanical analysis to derive the composite effective elastic moduli in terms of moduli of component phases, their volume fractions and morphology. These relations are then applied to the viscoelastic case by invoking the correspondence principle. The correspondence principle states that the effective complex moduli of a viscoelastic heterogeneous structure are found by replacing the phase elastic moduli by phase complex moduli in the expressions for the effective elastic moduli of an associated heterogeneous elastic specimen of identical phase geometry (1). The complex representation given earlier, namely, $\tilde{E} = E_0(1+i\eta)$, has at least two drawbacks. This representation has been found (3) to result in noncausal response if η were assumed independent of frequency. It has also been suggested (4) that the damping effect involves energy transformation between closely spaced vibration modes of a structure besides energy dissipation. Therefore eq. 1 is incomplete with respect to the total loss in energy because it involves only energy dissipation. The correspondence principle has been stated to be valid for relatively low frequencies of vibration of the structure (1). In spite of these drawbacks, the representation of eq. 1 has been used in conjunction with the correspondence principle widely to predict damping of composites .

Hashin (1,5) made an attempt to model the damping behaviour of composites, from a knowledge of the damping behaviour of the component phases and their volume fractions. In this approach it was assumed that the correspondence principle stated above was valid, and that the relationships amongst elastic moduli holds amongst complex moduli. The effective elastic moduli of a particulate composite were derived using the composite spheres assemblage model. The loss factors obtained by this model were found to be in agreement with experimentally determined loss factors of a silica sand embedded epoxy composite.

Hashin (5) derived the expression for complex modulus of composites with unidirectional fibers as shown in Figure 1a. The derivation was based on the composite cylinder assemblage model of Hashin and Rosen (6). It is to be noted that for the configuration Figure 1a, the longitudinal strain of fibers and of matrix will be the same. The assumptions in this analysis include: i. the matrix is transversely isotropic, and ii. the interfaces are perfect. To begin with Hashin (5) used the following expression for effective axial elastic Young's modulus for a composite where the poisson's ratios of the matrix and fiber are the same

$$E_a^* = E_1 v_1 + E_2 v_2 \quad \text{.... 5}$$

where E_a^* is the effective elastic Young's modulus, v_1 and v_2 are the matrix and fiber volume fractions and E_1 and E_2 are the matrix and fiber youngs moduli. Then the correspondence principle was invoked to obtain the expression for the effective complex Young's modulus, which is as follows :

$$\tilde{E}_a^* = \tilde{E}_1 v_1 + \tilde{E}_2 v_2 \quad \text{.... 6}$$

where the elastic Young's moduli in eq. 5 have been replaced by their complex counterparts in the form given in eq. 1.Recently Ankem and Kannan (7) have obtained an expression for the complex axial young's modulus of a composite beam with fibers oriented in the transverse direction as shown in Figure 1b. The assumptions in their analysis included those stated for the case of longitudinal fibers with the additional assumption that end effects are negligible. They (7) started with the expression for effective young's modulus of a composite where constant stress condition is assumed to be valid :

$$1/E_a^* = v_1/E_1 + v_2/E_2 \quad \text{.... 7}$$

Then invoking the correspondence principle, they derived an expression for the effective complex young's modulus. From this expression, an expression for loss factor was obtained which is as follows :

$$\eta^* = \frac{(\eta_1 v_1 E_2 + \eta_2 v_2 E_1 + \eta_1^2 \eta_2 v_2 E_1 + \eta_2^2 \eta_1 v_1 E_2)}{(v_2 E_1 + v_1 E_2 + \eta_1^2 v_2 E_1 + \eta_2^2 v_1 E)} \quad \text{.... 8}$$

It is realized that the constant stress assumption employed in the derivation of eq. 7 is not strictly valid because end constraints, are in general, not negligible . Nevertheless, eq. 8 can be used to get a rough estimate of the damping of composites with fibers in the transverse direction. The loss factors of various Al-epoxy composites were calculated based upon the Hashin's theory, i.e., eq 1, and for the perpendicular fibers, i.e., from eq. 8. These loss factors are plotted as functions of volume fraction of aluminum in Figure 2. The two assumptions obviously give distinctly different loss factors for the composites. Constant strain predicts much lower damping than constant stress assumption. In a broad sense these two assumptions can be treated as lower and upper bounds for loss factors respectively.

Based on elementary beam theory, Schultz and Tsai (8)

have derived a two dimensional transformation relation to determine the off-axis properties of a composite lamina or single ply in terms of the on axis properties. Subsequently, a micromechanics analysis was used to determine overall loss factors and moduli of a multi-ply laminate beam composed of unidirectional plies oriented in different directions. Comparison of composite moduli obtained from these analytical relationships with those obtained experimentally indicated that these analyses predict storage moduli accurately but they under predict loss modulus. This difference was attributed to the existence of a more complex state of stress in the individual laminae, especially close, to ply faces, than is assumed in analysis leading to derivation of composite beam effective moduli.

Gibson and Plunkett (9) approached the analysis of complex modulus of multi-ply laminates slightly differently. To begin with they obtained the effective elastic transverse and longitudinal moduli of a unidirectional continuous fiber composite lamina using the Hashin and Rosen model. Fibers were assumed nondissipative. Further, the effective elastic flexural modulus E_c was obtained from the engineering beam theory. In this theory , the following assumptions were made :

i. the beam is in pure bending

ii. loading of each ply is uniaxial along longitudinal axis

iii. each ply has a linear constitutive relationship .

This theory leads to an overall constitutive equation given by:

$$1/\rho = M / (E_c I) \qquad \text{....9}$$

where ρ is the beam curvature and E_c its flexural modulus. From this theory, the flexural modulus was derived to be :

$$E_c = 8/N^3 \left[E_0/8 + \sum_{j}^{(N-1)/2} E_j (3j^2 - 3j + 1) \right] \qquad \text{.... 10}$$

where N = number of plies, E_0 is the extensional modulus of the middle ply, E_j are the transverse / extensional modulus of the jth ply. The complex form of E_c is established by invoking the correspondence principle. Experiments were done to validate the micromechanical analysis for longitudinal and transverse complex Youngs modulus for one lamina and also for complex flexural modulus for a laminated composite. Micromechanics predicted flexural loss moduli that were lower than experimentally determined values, probably due to not considering the dissipative properties of fibers. Flexural storage moduli predicted by the model were, however, close to experimentally determined values.

The general principles outlined above, involving the use of the correspondence principle, were used to study the effective damping properties of short fiber reinforced composites and composite laminates (10, 11). The influence of fiber aspect ratio and orientation of fiber axis of a lamina with respect to loading direction are critically examined. It was concluded that (11) fiber orientation controls damping of a composite more effectively than fiber aspect ratio.

Sun, Wu and Gibson (12) applied the classical lamination theory, in conjunction with the force balance method and correspondence principle, to study damping of laminated composites as a function of fiber aspect ratio, fiber orientation , volume fraction and fiber and matrix damping properties. Force balance method was used to derive expressions for E_L, E_T, η_{LT} and G_{LT}, the longitudinal young's modulus, transverse young's modulus, poisson's ratio and shear modulus respectively, for an elastic unidirectionally oriented shortfiber lamina. This study did not take interlaminar stresses into consideration. Also , the unidirectionally oriented short fibers were of rectangular shape and were arranged in a rectangular array in the force balance derivation.

Apart from the above methods which are based on micromechanical analysis and the correspondence principle, a number of investigators have also used the correspondence principle in conjunction with differential equations of motion for laminated , multi-layered or sandwich plates (13-15). These differential equations were solved exactly or approximately for specific boundary conditions. Alam and Asnani (13) derive the governing differential equations of motion for the vibration of a multilayered orthotropic plate laminated composite. The in-plane displacements and excitation force were assumed in series form in terms of product of sines and cosines. Substitution of these series solutions in the differential equations yielded simultaneous algebraic equations for calculating the series coefficients. Correspondence principle was used to substitute complex properties for alternate layers and the simultaneous equations were reduced to eigenvalue problem form. Resonating frequencies and associated loss factors were determined. This procedure, which is a refined analysis that takes extension, bending and shear in all layers into consideration, could be applied to laminated plates with composite plies.

Cederbaum and Aboudi (14)used differential equations based on three shear deformation theories to study frequency response of a laminated plate containing unidirectional fiber plies. The five composite effective material constitutive functions in the time domain necessary for solution of these equations were obtained by inverse Fourier transformation of the corresponding frequency dependent functions. These composite frequency dependent functions, in turn, were obtained from a micromechanical analysis that starts from a Fourier transform of the time domain Boltzman representation of the viscoelastic behaviour of individual phases. The approach of Lifshitz and Leibowitz (15) was based on solving a sixth order differential equation of motion for a three layer sandwich beam where the midlayer is viscoelastic . The viscoelastic response of the midlayer in shear was accounted for by complex shear modulus . Composite damping loss factor corresponding to each natural mode of vibration is obtained from this (15) analysis which was then used in a computer program to optimize composite design .

The application of the correspondence principle in con-

junction with a two dimensional micromechanical analysis for determination of effective elastic properties is questionable since the state of stress at any interface with a viscoelastic layer is more complex than is accounted for in elastic analysis (16,17). This problem may be remedied to an extent by doing a far more complicated three dimensional analysis. Apart form this problem, which exists at perfectly bonded interfaces, imperfectly bonded interfaces may themselves be viscoelastic in their response. Hence their constitutive behaviour has to be characterised before their effect can be incorporated in modeling. Another estimate of damping is given by the quantity called damping capacity. Damping capacity or specific damping capacity is the ratio between energy dissipated and the strain energy stored in a particular deformation mode. Energy stored or dissipated is calculated using the stress and strain fields in a composite structure and the damping characterestics of the component phases. Modal damping capacity for a particular vibration mode is obtained from the amplitudes of the stress and strain fields in the body vibrating in that mode and the damping characterestics of the component phases. Since damping capacity calculation is based on strain energy in the composite structure, this approach is referred to as the strain energy or modal strain energy approach.

The strain energy approach was utilized in the determination of damping capacity of composites by many investigators (18-22). Adams and Bacon and Bacon (18,19) studied the damping of composite laminates made of unidirectional plies. Energy dissipation was divided into three parts relating to shear, longitudinal and transverse stresses. Their analytical approach did not predict damping for beams which had a complex lay up. Adams and Ni (20) made an attempt to improve this by application of laminated plate theory of Tsai (23) which allowed calculation of the elements of the overall laminated composite flexural modulus matrix in terms of the elements of the stiffness matrix of a unidirectional fiber reinforced composite lamina. For vibration in first flexural mode, the stresses and strains along global x and y axes and xy direction (see Figure 3 for schematic of laminated composite and the coordinate system used in the analysis) for the kth layer were determined in terms of the stiffness matrix elements of the kth layer and applied flexural moment. The stiffness matrix of the kth layer which was at an angle θ to the longitudinal direction of the composite , was obtained from the on axis stiffness elements through transformations. The experimentally determined ψ_L, ψ_T and ψ_{LT} , which are the longitudinal, transverse and shear damping capacities, respectively for a lamina with longitudinally oriented fibers, were also transformed to a direction rotated by angle θ from the longitudinal direction. From this analysis ΔZ_x, the energy dissipated in the x direction due to damping, is given by

$$\Delta Z_x = 2\int_0^{y_2}\int_0^{x_2}[2\int_0^{1/2}\psi_L \sigma_x \varepsilon_x dz]\, dx \qquad \ldots 11$$

ΔZ_{xy} and ΔZ_y are computed from similar formulae. The damping contribution of the stresses and strains in the x direction, ψ_x, to the total damping capacity ψ is given by

$$\psi_x = \Delta Z_x / Z_x \qquad \ldots 12$$

The quantities ψ_y and ψ_{xy} can be got in a similar fashion. The damping capacities of various laminated composites determined from these analyses were found to be in excellent agreement with those obtained experimentally. As described above, most of the analytical solutions are applicable in general for specific configurations and geometries of the composites. In addition, most of these analytical solutions cannot take such factors as the interface effects into consideration. Therefore the application of these models is limited. The numerical methods which are discussed in the next section do overcome many of the shortcomings of these analytical methods.

Numerical Methods. The analytical methods described in the preceeding section are limited in scope and in general they are applicable only to specific and simple geometries. In this regard, numerical methods such as the finite element method (FEM) appear to be attractive because they can be applied to complicated geometries.

The finite element form of the equation of motion of a structure at a given instant of time can be written as (24) :

$$[M]\{\ddot{u}\} + [C]\{\dot{u}\} + [K]\{u\} = \{F_{ext}\} \qquad \ldots 13$$

where [M], [C] and [K] are the mass, damping and stiffness matrices of the structure, $\{\ddot{u}\}$, $\{\dot{u}\}$ and $\{u\}$ are the vectors of nodal acceleration, velocity and displacement and $\{F_{ext}\}$ is the vector of external nodal loads, respectively. In general, the dynamics problems can be classified as shown in Figure 4.

The methods for analysis of damping of structures based on eq. 13 can be grouped into four categories :

1. Direct transient response analysis : This is a means of obtaining the time history of the nodal displacement vector {u}. A finite difference time marching scheme (24) is used in conjunction with the spatial discretization given in eq. 13 to obtain the time history of {u}. For a given composite structure, effective loss factor can be obtained from this time history by determining the time lag between an applied nodal load and the displacement response of the structure at that node. The entire computation is done in the time domain for a particular frequency of the applied external load . The loss factor so determined is specific to that frequency. In this scheme , establishment of the [C] matrix poses the biggest problem. Several approximations are used in order to reduce computational effort in the analysis.

2. Complex eigenvalue analysis (25) : Complex eigenvalue analysis is computationally much more expensive for the determination of loss factors than direct transient analysis. In this method, damped natural frequencies of vibration and corresponding mode shapes are determined and the effective loss factors of the com-

posite can be obtained for each natural frequency. This analysis may be carried out in two ways :

a. The analysis can be carried out using the homogeneous form of the eq. 13. In this approach , the establishment of the [C] matrix and the heavy computational cost involved are the main problems , and

b. alternatively, if the properties of the component phases are known in complex form, eq. 1, the structural stiffness matrix can also be established in complex form, i.e., $([K_1] + i[K_2])$. The [C] matrix in the homogeneous form of eq. 13 may then be ignored in this eigenvalue analysis. This scheme is also computationally expensive. Frequency dependent loss factors can be established from the damped natural frequencies .

3. Direct Frequency response analysis (25) : For a harmonic external nodal load vector, for example $\{F_{ext}\} = \{L(\omega)\} \sin\omega t$, the displacement response, $\{u\}$, is assumed to be harmonic, i.e., $\{u\} = \{X\} \sin\omega t$. If the stiffness matrix is derived for the structure from the complex form of the constitutive properties, as in the scheme 2b., the eq. 13 can be transformed as :

$$[-[M]\omega^2 + [K_1(\omega)] + i[K_2(\omega)]]\{X\} = \{L(\omega)\} \quad .... 14$$

where, $\{X\}$ is the vector of displacement amplitudes and $\{L(\omega)\}$ the vector of nodal load amplitudes.

The imaginary term in eq. 14 results from the complex modulus representation. Direct frequency response analysis, involving the solution of eq. 14, leads to the determination of vibration response amplitude vector $\{X\}$ as a function of frequency ω. This also involves extensive computer time and memory since the impedance matrix which is the coefficient matrix of the vector $\{X\}$ in eq. 14 , has to be recomputed for each desired frequency.

4. Modal strain energy method (25) : This method is normally used in conjunction with the modal superposition scheme (24) to determine structural response for structures assumed to be damped by a linear viscous damping mechanism, for example the Rayleigh mechanism .

Complex eigenvalue analysis belonging to category 2a and complex frequency response analysis belonging to category 3, use frequency dependent moduli in conjunction with a form of eq. 13 in which the [C] matrix is ignored. Damped natural frequencies and loss factors determined by these analyses are quite accurate . However, since the use of these methods entails great computational expense, alternate methods were sought and developed. Therefore no further consideration is given to categories 2a and 3 further in this paper. Computation of the [C] matrix is central to the analysis of damping of a structure by the methods 1 and 2b. Determination of the [C] matrix that correctly represents damping of a structure is difficult and the different approaches available to do this are considered in this paper. In addition, analysis by category 4 is reviewed as they are attractive from a computational point of view.

The [C] matrix in approximate form is often expressed as a linear combination of [K] and [M] matrices. Such methods are called spectral damping methods. In spectral damping, viscous damping is represented by ξ which is defined as the ratio between observed structural damping c and the critical damping c_c which corresponds to structural damping that would give a nonoscillatory response. The damping ratio is dependent upon material, geometry of the structure and vibration frequency. A commonly used viscous spectral damping scheme is the Raleigh form given by :

$$[C] = \alpha [K] + \beta [M] \quad .... 15$$

where α and β are constants determined from the experimentally obtained damping ratio in the frequency range of interest. An illustration of the use of this form of [C] is given by Zabaras and Pervez (26).

When [C] is represented by Rayleigh viscous damping, the damping ratio ξ_i for the ith mode is given by :

$$\{\varphi\}_i^T [C] \{\varphi\}_i = 2\xi_i\omega_i, \quad .... 16$$

where $\{\varphi\}_i$ is the ith eigenvector corresponding to ω_i . For the case of forced harmonic vibration of a structure damped by Rayleigh viscous damping mechanism, the three damping measures, ψ_i, η_i and ξ_i, are interrelated as given below :

$$\psi_i = 4\pi\xi_i = 2\pi\eta_i \quad .... 17$$

For this case, damping capacity ψ_i is defined as the ratio between the energy absorbed in a cycle and the strain energy corresponding to the maximum displacement during the cycle at frequency ω_i. Similarly, loss factor η_i is defined as the ratio of the energy absorbed per radian to the strain energy at maximum displacement during the cycle. The above equation may be used even in the case of non-Rayleigh damping mechanisms to define an 'equivalent ' Rayleigh damping ratio.

Here, Zabaras and Pervez (26) used free vibration tests to extract damping characterestics of laminated composites. Frequency response and time history tests were carried out. Experimentally determined damping capacities of individual unidirectional laminae were used to determine average loss factors for the ith damping mode of the laminated composite structure. The mode shapes for the structure were obtained by eigenvalue analysis. The modal damping ratios were determined from experimentally determined damping capacities. These damping ratios are used with the eigenvalues computed earlier to determine α and β, eq. 14, for the frequency range. The [C] matrix so determined, eq. 15, was used for transient response analysis of laminated plate composite. Specific damping capacity of the composite obtained for different modes as a function of angle of the ply outer most layer was compared with experimentally determined values. Reasonable agreement was observed for the case where material damping was not high. The Rayleigh approximation cannot be em-

ployed in applications where the material damping is known to be large and for materials in which the viscous damping assumption is inappropriate. For the majority of structural materials, damping occurs by complicated internal friction mechanisms rather than by viscous means.

Realistic damping behaviour of composite structures necessitates the representation of [C] as a nonproportional damping matrix. Several investigators (27-29) describe the determination of appropriate structural nonproportional damping matrices. The general form of the nonproportional damping matrix is :

$$[C] = \alpha [K] + \beta [M] + \gamma [I] \quad \text{.... 18}$$

The [C] matrix can be obtained if α, β and γ can be determined .

Liang and Lee (29) represented the damping matrix, [C], as a polynomial of [K] and [M] matrices. Such a representation is shown to overcome the disadvantage of Rayleigh damping representation, namely that Rayleigh damping can yield only the normal modes of vibration of structure and not the complex modes. Some of the earlier attempts to represent nonproportional damping are detailedin the references (30-34).

Lee and Dobson (35) described a way for directly obtaining mass, stiffness and damping matrices of a structure based on experimental observations. They (35) have developed relationships to calculate the matrices from the results of frequency response and modal tests. The mass , stiffness and damping matrices obtained through finite element discretisation of a homogeneous body or of a composite structure may be reduced to match the size of matrices calculated from experimental results. The experimentally determined matrices (35) could serve two purposes - validation of finite element approximations of the damping matrix and establishment of a damping matrix for subsequent finite element analyses.

Saravanos and Chamis (36) devised a general scheme for determination of a structural damping matrix and thereby the modal specific damping capacity which is applicable to laminated beams, plates and shells. They derived a relationship for the determination of on-axis damping of a fiber reinforced composite lamina in terms of the properties of fiber and matrix and their volume fracions. Off-axis damping was calculated from these on-axis composite properties by applying their earlier micromechanics derivation (21) which was based on a strain energy method (total strain energy under a given deformation mode is the sum of contributions from constituent phases). These properties were used to formulate local laminate damping capacity. A special triangular multilayered laminated composite finite element was developed whose element damping matrix is derived from off-axis properties of individual laminae. The element damping matrix , $[\zeta_e]$, had extensional, bending and extensional-bending coupling contributions and was fully populated. The dissipated energy per cycle of deformation , ΔW_e, for a plate or shell element in harmonic vibration was given by

$$\Delta W_e = 1/2 \int_A \{\varepsilon_e\}^T [\zeta_e] \{\varepsilon_e\} dA \quad \text{.... 19}$$

Using the strain displacement relationship, $\{\varepsilon_e\} = [B_e]\{u_e\}$, where $[B_e]$ is the strain displacement matrix for the element e and $\{u_e\}$ is the corresponding displacement vector, this was be written as :

$$\Delta We = 1/2 \{u_e\}^T [\int_A [B_e]^T [\zeta_e] [B_e] dA] \{u_e\} \quad \text{.... 20}$$

Dissipated energy for the entire structure, ΔW, was obtained by assembling the element damping matrices $[\zeta_e]$ to get the structural damping matrix $[\zeta]$. The specific damping capacity ψ for the structure is given by

$$\psi = \Delta W / W \quad \text{.... 21}$$

where W is the structural strain energy. Thus, modal specific damping capacity was obtained by determining the dissipated and total strain energies for the structure from the mode shapes obtained from an eigenvalue analysis for the undamped natural vibrations. Finite element analysis was carried out to study variation of natural frequency and modal damping capacities as functions of laminated composite layup and fiber volume fraction.

The damping capacities determined by methods similar to (36) can be used to determine the loss factor etc. by eq. 17 for the case where the Rayleigh damping mechanism is applicable. The loss factor so determined are used in conjunction with the modal superposition method to obtain the transient response of a structure. Details of this method are given by Cook et al (24). Johnson and Kienholz (25) applied this method to predict the damping behaviour of composites. Here, eq. 13 , which has nodal displacements as the degrees of freedom at the nodes, is transformed into one in terms of generalised coordinates, α. This is done by a transformation whereby nodal displacements at any instant are given as a linear combination of undamped mode shapes $\{\varphi\}_i$:

$$\{u\} = [\varphi] \{\alpha\} \quad \text{.... 22}$$

where $[\varphi]$ contains all the mode shapes $\{\varphi\}_i$ of the undamped structure, and $\{\alpha\}$ thus represents a vector of "coefficients". This method thus involves the determination of the undamped mode shapes of a structure as a first step. When the transformation eq. 22 is substituted into eq.(13), the transformed equations are uncoupled for each mode provided a lumped mass formulation is used and the damping matrix is proportional to mass and stiffness. The typical decoupled equation for the rth mode is :

$$\ddot{\alpha}_r + \eta^{(r)} \omega_r \dot{\alpha}_r + w_r^2 \alpha_r = l_r(t) \quad \text{.... 23}$$

where $\eta^{(r)}$ is the loss factor of the structure in the rth mode . This loss factor is calculated by the modal strain energy method from

the loss factors of the component phases or by the procedure of (36) outlined earlier. If $V^{(r)}$ is the strain energy in the structure corresponding to the rth undamped mode , $V_v^{(r)}$ is the energy dissipated in all the viscoelastic phases of the structure and η_v is the loss factor of the viscoelastic phases, then $\eta^{(r)}$ is given by :

$$\eta^{(r)} = \eta_v [V_v^{(r)} / V^{(r)}] \quad \text{.... 24}$$

This method is computationally much less expensive than the complex eigenvalue analysis and the complex frequency response analysis described earlier as it entails the computation only of normal (undamped) modes of the structure. However, the Rayleigh damping approximation assumed for reducing computational cost allows it to be used only for lightly damped structures. Moreover, calculation of modal strain energy $V^{(r)}$ from the undamped mode shapes involves the use of frequency independent moduli for all the component phases (25). While this frequency independence is a valid condition for elastic materials, the storage moduli of viscoelastic materials are known to be functions of frequency. This problem was rectified (25) by empirical corrections to the computed loss factors depending on the geometry of the composite structure. Sandwich beams and rings and plate configurations for which analytical or other approximate solutions are readily available were modeled by the strain energy approach using MSC/Nastran . Modification of modal loss factors (25) with appropriate empirical corrections yielded results that were found to be close to those obtained by more expensive methods such as eigenvalue analysis. Several investigators have applied the modal strain energy method to different composite modeling problems (37-39).

Kubomura (40) reported another way of dealing with nonproportional damping. When damping is nonproportional, the second order equations of motion, eq. 13 , do not get uncoupled when transformed into modal coordinates. So, the second order equations are converted into first order equations for nodal velocities. From the decoupled modal equations thus obtained , modal coordinates, and subsequently velocities, are solved for. These solutions were used to synthesize solutions for problems with three different boundary conditions (40).

The various methods discussed so far arise from the context of eq. 13. Conventional methods, in dealing with eq. 13, need some simplifying assumptions like proportional damping behaviour in order to reduce complexity of the problem and to enhance computational efficiency. There have been attempts to model structural damping which were not based upon eq. 13 .

Outside the context of eq. 13, special composite finite elements have been formulated that incorporate the overall viscoelastic response of the composite. Lin and Hwang (41) started by expanding an existing functional for viscoelastic materials to include nonisothermal effects. They incorporated the integral form of the linear , time and temperature dependent viscoelastic constitutive equation in the functional and minimised it to obtain the equilibrium equations for an element. The constitutive equation was that of single fiber reinforced lamina. Based on the above equation for a single ply, a multi-ply finite element was developed whose stiffness matrix was defined in terms of the constitutive functions of the individual plies. The global finite element equations assembled from element stiffnesses is of the form

$$\int [K]\{u\}\, dt = \{F_{ext}\} \quad \text{.... 25}$$

The integration in the equation was done by approximate means. As can be seen from eq. 25, this method did not include material inertia effects and was used to obtain time dependent stress- strain fields in alminated composite. However, by appropriately expanding the functional , material inertia effects may also be included so that the equations developed can also be used to study dynamic problems.

Douven et al (42) presented another constitutive equation for unidirectional fiber composite plates where both fiber and matrix were considered viscoelastic. The viscoelastic relaxation function in the constitutive equations were obtained from those of the fiber and matrix using micromechanical analysis based on the Hashin and Rosen model. Dynamic finite element equations were derived for an element utilizing the above constitutive equations. This finite element formulation was used to obtain the effect of fiber orientaion on the evolution of stresses in a membrane structure. This formulation could also be used to determine loss factors for such membrane structures.

The form/ structure of eq. 13 has been criticised as being incapable of providing a macroscopic representation of the actual microscopic material damping mechanisms over a broad frequency range (43). Lesieutre and Mingori (43) outlined a new approach for modeling the internal dissipation in a material which is based on the augmenting thermodynamic field concept. This approach is illustrated below for the case of longitudinal vibrations in a rod. Energy dissipation in the material of the rod was characterised by an internal field variable $\zeta(x)$. The coupling between the internal field $\zeta(x)$ and the displacement field $u(x)$ in the material was given by δ, a material property. The $\zeta(x)$ was related linearly to an affinity factor A through α. The helmholtz free energy density in the body was defined as :

$$f = 1/2E\varepsilon^2 - \delta\varepsilon\zeta + 1/2\alpha\zeta^2 \quad \text{..... 26}$$

where E is axial Young's modulus and ε is strain .
The material constitutive equations were given as

$$\sigma = E\varepsilon - \delta\zeta$$

and

$$A = \delta\varepsilon - \alpha\zeta, \quad \text{.... 27 a, b}$$

where σ is the stress field in the rod.
The equations for evolution of the field variables were

$$\rho\ddot{u} - E u'' = -\delta \zeta'$$

$$\dot{\zeta} + B\zeta = (Bd/\alpha)u' \quad \text{.... 28 a, b}$$

where B is a relaxation constant. Under appropriate conditions,

the governing equations represent the dissipative nature and the solution is dependent on initial conditions. The approximate damping ratio was determined to be frequency dependent and was
given as

$$\xi = 1/4(\delta^2/E\alpha)(2(\omega/B))/(1+(\omega/B)^2) \quad \text{....29}$$

The above frequency dependence was found to be closer to observed levels for several microstructural damping mechanisms. From the governing evolution equations, a coupled finite element formulation was derived and the associated eigenvalue problem was solved for the natural vibration frequencies and modes of the rod. A coupled finite element formulation was derived using eqs. 26, 27 and 28 with u and $d\zeta/dx$ as independent variables and the corresponding eigenvalue problem was solved . System equations were also derived for transverse vibration of a beam and for vibration of a planar space truss and the eigenvalue analyses carried out.

In a further relatively unconventional attempt to model damping of laminated plates, Ba and He (44) formulated a new finite element based on the asymptotic solution method for harmonic flexural vibrations of viscoelastically damped sandwich plates. The formulation of the finite element equations was based on the discrete kirchoff thoery. This formulation was then appropriately transformed for eigenvalue analysis. The finite element equation formulation assumed only elastic behaviour. Viscoelastic behaviour was introduced into the equations for eigenvalue analysis through the correspondence principle. Complex frequencies and mode shapes were determined through the analysis. They (44) reported that these complex characteristics are more accurate than those obtained from the modal strain energy method. Even though this approach (44) improved accuracy it appears that it is applicable only to simple plate geometries. Its application to laminated plate composite structures has not been studied.

The relative advantages and disadvantages of the four common techniques of numerical analysis of damped structures may be summarised as follows . The direct transient response analysis scheme is most appropriate for determining composite structural response in the time domain and also to determine composite loss factor for different frequencies. Since this employs an approximate time integration scheme based on finite difference method in the time domain, it is relatively inexpensive. However, characterization of the damping of the composite structure through an appropriate [C] matrix poses the greatest problem in this case since realistic material damping would have to be represented by a non-proportional damping matrix. Nanavaty and Ankem [45] used the direct transient response analysis method to study the damping behaviour of particulate composites and unidirectional fiber composites loaded in the transverse and longitudinal directions. Cosmic/Nastran finite element analysis package was used for this study. This code approximates the damping matrix as the sum of linear functions of the element stiffness matrices, each of the element stiffness matrices being expanded to global dimension prior to summation (46). Predicted loss factors were found to be consistent with the experimental trends obtained by various investigators for continuous fiber composites. A typical mesh used by Nanavaty and Ankem (45) is shown in Figure 5.

The complex eigen value analysis (47) based on the complex moduli can predict loss factors and damped mode shapes accurately but is computationally expensive. This is also true of complex frequency response analysis. For both these schemes, establishment of frequency dependent complex moduli is very important. Experimental methods for the establishment of viscoelastic constitutive behaviour and frequency dependent moduli are well established (48-54).

The modal strain energy method in conjunction with the modal superposition method is inexpensive but as outlined above, there are problems associated with this and may not be applicable in its present form to determining the damping behaviour of structures with high damping.

Modeling of Active Damping

Increasing the passive damping of composite structures through optimisation of the component phases may not be sufficient for instances involving large vibrational deformations. Such instances include vibration control in large space structures (eg., satellite antennae), aircraft structures and helicopter rotor blades , buckling prevention in plates and fatigue damage reduction (55, 56). In addition, enhancement of passive damping may require compromising in the stiffness and strength requirements of a structure. For these cases active damping has to be considered . In the active damping technique energy is infused into a structure only at the desired point of time for suppression of vibrational deformation. The actively damped structure has to be part of an "intelligent" or "smart" system that integrates sensing of deformation, actuation (infusion of energy into the structure) and control of actuation.

Sensing and actuations have to be done without altering structure properties significantly and adversely. Piezoelectric materials, optical fibers and magnetostrictive materials are suitable for sensing applications. Actuation may be achieved by use of shape memory alloys , piezoelectric materials and magnetostrictive materials.

The application of piezoelectric materials for active vibration control has been widely studied experimentally (55, 57-59) and modeled analytically (57) and numerically using FEM (55, 60-63).

The finite element equations for the analysis of composite structures containing piezoelectric actuators may be derived from variational principles (60-62) or by using Hamilton's principle (63). Modeling studies have so far been done on simple configurations such as plate, beam and simple truss structures. While the numerical models developed so far for simple applications have

withstood the test of experiments, application of these models to complicated, highly integrated smart systems depends on the development of numerical techniques for coupling the control problem to the structural analysis problem and on the development of efficient control algorithms (56).

Magnetostrictive materials of high force and actuation capability are of recent development. Terfenol - D , a rare earth iron alloy containing terbium and dysprosium is the material that produces highest magnetostriction. However, it has not been as widely studied experimentally in active damping control applications as piezoelectric materials have been. One reported example of the application of magnetostrictives to active damping is the use of Terfenol-D as the legs of an optical table (64). Vibrations of the table top are actively damped off by appropriate bending of the terfenol legs. Magnetostriction properties i.e., the actuation strain versus applied magnetic field, are nonlinear and sensitive to manufacturing conditions, applied bias magnetic field and prestress. It is probably due to this complexity that the coupled magnetomechanical effect has not been modeled, by FEM or analytical methods, in the context of applications to damping of structural vibrations as much as the electromechanical effects.

Shape memory alloys (SMA) provide high force large strain actuation but have poor frequency response. Their inherent hysteretic nature provides additional passive damping. SMAs have great potential for applications to damp low frequency vibrations in large structures. Special materials and analytical models are being developed with space applications in view (65).

Active damping or vibration control of structures is a relatively new area of research with enormous scope for numerical and analytical model building.

Future Developments

In the view of the authors, great scope for future work exists in four areas in regard to modeling of damping behaviour of composites.

The first area relates to the modeling of the damping behaviour of particulate composites. Modeling of particulate composites requires a three dimensional approach. Effect of particle morphology, distribution and volume fractions needs to be systematically studied.

The second area is related to interface effects. Interfaces or interphases between component phases in a composite are very important features that affect overall composite behaviour. Interphase may represent coatings on the fiber or particles, chemical interdiffusion zones, weak layers of imperfect bonding between phases or inelastic regions in metal matrix composite. Interphases usually behave in a viscoelastic manner even if parent phases are elastic. Interphases give rise to three dimensional stress states at the junction with matrix or fiber. Effect of interface on damping properties has been studied using simple analytical models for simple geometries based on the force balance and energy balance (for example, 66). Also, simple interface / interphase models are available (67,68) . However, future developments in this area are expected to include the nature of the interphases and interfaces in numerical and analytical models in three dimensional analysis.

The third area of future interest is related to the establishment of methods for identification of realistic nonproportional damping matrices for use in finite element structural models.

The fourth area is related to the modeling of active damping. While the finite element formulation for piezoelectric materials embedded in a composite structure have been established, its applicability has to be tested for large scale complicated structures. The effect of interfaces also needs to be incorporated. For structures incorporating magnetostrictive materials or shape memory alloys, deformation models need to be established that couple the magneto-mechanical and thermo-mechanical effects, respectively.

Summary

In regard to modeling of passive damping , in general, analytical methods can be applied only to relatively simple geometries and composite configurations. Even for simple cases, analytical methods developed are usually specific to geometry and configuration. However, numerical methods, especially FEM, have the potential for application to arbitrary composite geometry and configuration and arbitrary loading conditions.

Active damping can enhance damping capability significantly without affecting the other properties of the structure. Modeling of active damping poses the challenge of coupling the mechanical field with the electrical, thermal and magnetic fields.

References

1. Hashin, Z., Int. J. Solids Structures 6, 539-552 (1970)
2. Gaul, L., Klein, P. and Kempfle, S., in Proceedings Damping '89, W.Palm Beach, FL, Feb 1989, p. DCD 1 - DCD 11
3. Christensen, R. N., "Theory of Viscoelasticity", Academic press, New York(1971)
4. Tong, M., Liang, Z. and Lee, G.C., in Proceedings Ninth Intl. Modal Anal. Conf., Firenze, Italy, Apr. 1991, p.1509-1514
5. Hashin, Z., Int. J. Solids Structures 6, 797-807 (1970)
6. Hashin, Z. and Rosen, B.W., J. Appl. Mech. 31, 223 (1964)
7. Ankem, S. and Kannan, K.S., Unpublished Research (1992)
8. Schultz, A. B. and Tsai, S. W., J. Comp. Materials 3, 434(1969)
9. Gibson, R. F. and Plunkett, R., J. Comp. Materials 10, 325 (1976)
10. Sun, C. T., Chaturvedi,S. K. and Gibson, R. F., Computers and Structures 20, 391 (1985)
11. Suarez, S. A., Gibson, R.F., Sun, C. T. and Chaturvedi,S. K., Experimental Mechanics, 175 (1986)
12. Sun, C. T., Wu, J. K. and Gibson, R.F., J. Mats. Sci. 22, 1006 (1987)
13. Alam,N. and Asnani, N. T., J. Sound & Vibration 119, 347 (1987)

14. Cederbaum, G. and Aboudi, J., J. Sound and Vibration 113, 225 (1989)
15. Lifshitz, J.M. and Leibowitz, M., Int. J. Solids Structures 23, 1027 (1987).
16. Vallianos, C., Comp. Sci. & Tech.30, 239 (1987)
17. Milios, J. and Spathis, G., Comp. Sci. & Tech. 25, 301 (1986)
18. Adams, R. D. and Bacon, D. G. C., J. Comp.Materials 7,402 (1973)
19. Bacon, D. G. C., "The Dynamic Properties of Carbon and Glass Fiber Reinforced Plastics." Ph. D. Thesis, University of Bristol, (1973)
20. Ni, R. G. and Adams, R. D., J. Comp. Materials 18, 104 (1984)
21. Saravanos, D. A. and Chamis, C. C., J.Comp. Tech.& Research 12, 31 (1990)
22. Lee, C.Y., Pfeifer, M., Thompson, B.S. and Gandhi, M. V., J.Comp. Materials 23,819 (1989)
23. Tsai, S.W., "Structural Behaviour of Composite Materials," NASA, CA 71 (1974).
24. Cook, R.D., Malkus, D.S. and Plesha, M.E., "Concepts and Applications of Finite Element Analysis" , Third Edition, Chap. 13, JohnWiley & Sons Inc.(1989)
25. Johnson, C.D. and Kienholz, D.A., AIAA Journal 20,1284 (1982)
26. Zabaras,N. and Pervez,T., Computer Methods in Applied Mechanics and Eng. 81, 291 (1990)
27. Ma, X., Liang, Z. and Lee, G.C., in Proceedings Ninth Intl. Modal Anal. Conf., Firenze, Italy, Apr. 1991, p. 1375-1380
28. Minas, C. and Inman, D.J., J. Vibration & Acoustics 113, 219 (1991)
29. Liang, Z. and Lee, G.C., J Eng. Mechanics 117, 1005 (1991)
30. Berman, A., and Nagy, E.Y., AIAA Journal 21, 1168-1173 (1983)
31. Golla, D.F., and Hughes, P.C., J. App. Mech. 50, 897-906 (1985)
32. Buhariwala, K.J., and Hansen, J.S., J. App. Mech. 55 , 443-447 (1988)
33. Mau,S.T., Earthquake Eng. Structural Dynamics 16, 931-942 (1988)
34. Caravani, P., and Thomson, W.T., J. App. Mech. 41, 379-392 (1974)
35. Lee, H.G. and Dobson, B. J., J. Sound & Vibration 145, 61 (1991)
36. Saravanos,D.A. and Chamis,C.C., J. Reinforced Plastics and Comp. 10, 256 (1991)
37. Hwang, S. J. and Gibson, R. F., Comp. Sci. and Tech. 41, 379 (1991)
38. Parekh, J. C. and Harris, S.G., in Proceedings Damping '89, W.Palm Beach, FL, Feb 1989, p. CCB 1 - CCB 28.
39. Saravanos, D.A. and Chamis, C. C., AIAA Journal 30,805 (1992)
40. Kubomura, K., AIAA Journal, 25, 740 (1987)
41. Lin, K. Y. and Hwang, H., J. Comp. Materials, 23, 554 (1989)
42. Douven, L. F. A., Schreurs, P. J. G. and Janssen, J. D., Int. J. Numerical Methods in Eng. 28, 845 (1989)
43. Lesieutre, G. A. and Mingori, D. L., J. Guidance 13, 1040 (1990)
44. Ma, B.A. and He, J. F., J. Sound & Vibration 152, 107 (1992)
45. Nanavaty, A. and Ankem, S., The Effect of Morphology and Volume Fraction on the Damping of Epoxy/Aluminum composites, unpublished research, 1992
46. The Cosmic / Nastran Theoretical Manual, Chap. 9, NASA, D.C, Jan 1981
47. Soni, M. L. and Bogner, F. K., AIAA Journal 20, 700 (1982)
48. Lin, C. H. and Plunkett, R., J. Comp. Materials 23, 92 (1989)
49. Updike, C. A., Bhagat, R. B., Pechersky, M. J. and Amateau, M. F., J. Metals , 42 (1990)
50. Rogers, J. D., Zachary, L. W. and McConnell, K. G., Experimental Mechanics, 283(1986)
51. Andriulli, J. B.in Proceedings Damping '89, W.Palm Beach, FL, Feb 1989, p. BCC 1- BCC 26
52. Pundit, S. M. in Proceedings Damping '89, W.Palm Beach, FL, Feb 1989, p. CBB 1 - CBB 11
53. Crane, R. M. and Gillespie, Jr. J. W., Comp. Sci & Tech. 40, 355 (1991)
54. Crane, R. M. and Gillespie, Jr. J. W.,J. Comp. Tech. & Research 14, 70 (1992)
55. Preumont,A., Dufour, A.-J., and Sparavier,M., in "Dynamics of Flexible Structures in Space", p.369, C.L.Kirk and J.L.Junkins, eds., Springer-Verlag, 1990
56. Thompson, D. M. and Griffin Jr. O. H.,in Proceedings of conference on Recent Advances in Adaptive and Sensory Materials and their Applications, 1992, p.377-384
57. Hagood, N. W., Chung, W. H. and Flotow, A. V., J. Intel. Mater. Syst.& Structures 1, 327 (1990)
58. Im, S. and Atluri, S. N., AIAA Journal, 1801 (1989)
59. Wang, B. T. and Rogers, C. A., J. Intell. Mater. Syst. & Structures, 2, 38 (1991)
60. Ha, S. K., Keilers, C. and Chang, F. K., J. Intell. Mater. Syst. & Structures 2, 59 (1991)
61. Ha, S. K., Keilers, C. and Chang, F. K., AIAA Journal 30, 772 (1992)
62. Krishna, M. R. M. and Mei, in Proceedings of conference on Recent Advances in Adaptive and Sensory Materials and their Applications, 1992, p.301-313
63. Tzou, H. S. and Tseng, C. I., J. Sound & Vibration 138, 17 (1990)
64. Greenough, R. D., Jenner, A. G. I., Schulze, M. P. and Wilkinson, A. J., J. Magnetism and Magnetic Materials 101, 75 (1991)
65. Maclean, B. J., Patterson, G. J. and Misra, M. S., J. Intell. Mater. Syst. &. Structures 2, 72, (1991).
66. Chaturvedi, S. K. and Tzeng, G. Y., Proc. of Am. Soc. for Comp. Fifth Technical Conference, June 12-14, 1990, E. Lansing, MI, p. 1044-1053
67 J.ayaraman, K., Gao, Z. and Reifsnider, K. L.,Proc. of Am. Soc. for Comp. Sixth Technical Conference, p.759-768
68. Gao, Z. and Reifsnider, K. L., Proc. of Am. Soc. for Comp. Sixth Technical Conference, p. 742-752

Acknowledgements

The authors would like to thank Dr. Larry Kabacoff of the Office of Naval Research and Mr. Ivan Caplan of CD/ NSWC for their encouragement and support. This work is being funded by the ONR under contract number N 00014-92-J-4039.

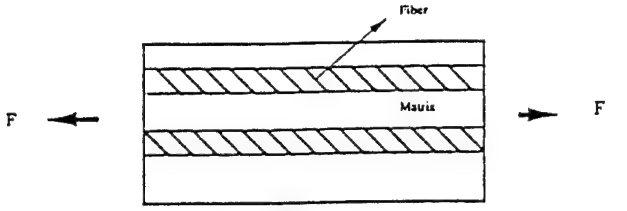

(a) Composite loaded in direction of fiber length ; here longitudinal strain may be assumed to be same in fiber and matrix [7]

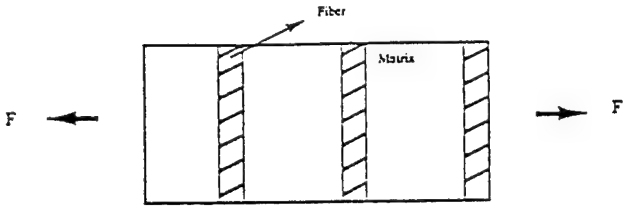

(b) Composite loaded perpendicular to fibers; here stress is the same at any cross section [7]

Fig. 1 : Composite configurations used in analyses [5,7]

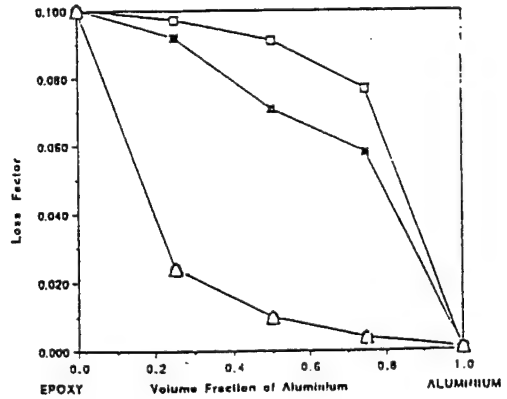

transverse fibers, constant stress assumption (7)

transverse fibers, FEM (45)

longitudinal fibers, constant strain assumption (5)

longitudinal fibers, FEM (45)

Fig. 2 : Comparison of loss factors of unidirectional composites obtained by analytical methods based on constant stress assumption (5) and constant strain assumption (7) and the FEM method (45)

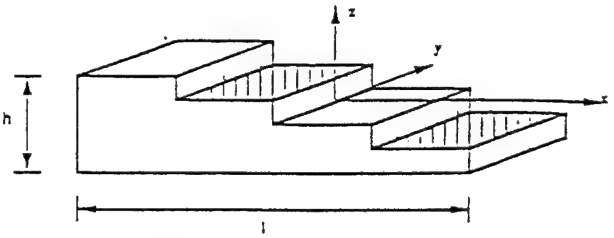

Cut away view of plies in a multi-ply laminated composite beam; coordinate axes used in analysis are also shown

Fig. 3 : Layup of laminated beam used in analysis [20]

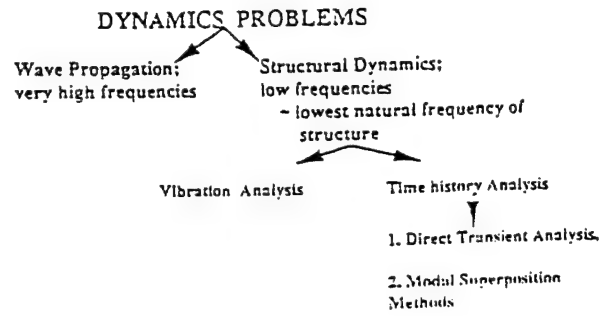

Fig. 4 : General classification of dynamics problems based on FEM solution methodology

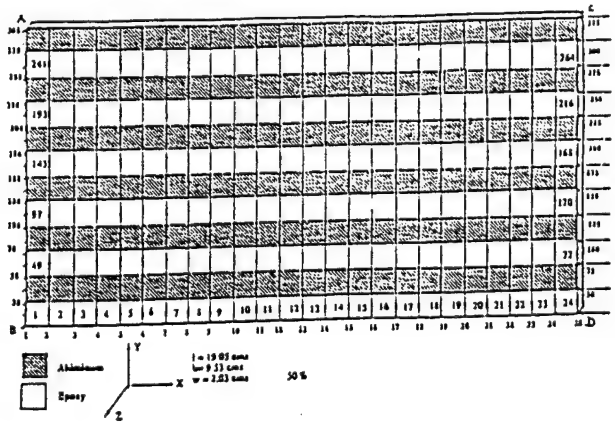

Fig. 5 : A typical mesh used in FEM analysis of damping behaviour of Al-epoxy composite by Nanavaty and Ankem (45)

2B. TECHNICAL PROGRESS : PART II

THE EFFECT OF MORPHOLOGY AND VOLUME FRACTION ON THE DAMPING OF EPOXY/ ALUMINUM COMPOSITES

Aashish Nanavaty and Sreeramamurthy Ankem
Department of Materials and Nuclear Engineering
University of Maryland
College Park,MD 20742-2115, U.S.A

Abstract

To design composite materials with high intrinsic damping, it is essential to understand the effect of volume percent and morphology (size, shape, orientation and distribution) of the component phases on the damping behavior. Available analytical solutions are primarily concerned with specific morphologies and thus cannot predict the result of a change in the morphology of the component phases even though they account for volume percent effects. In this investigation the Finite Element Method (FEM) has been used to predict the effect of both volume percent and morphology of phases on the damping behavior of Epoxy-Aluminum composites. It was found that the loss factors of composites with Al or Epoxy fibers perpendicular to the loading direction are much higher than those with fibers parallel to the loading direction. This was attributed to the constrained deformation in the latter case. Furthermore, the loss factors of composites with particles of Al or Epoxy depending on the volume fraction, were found to be in between those of parallel and perpendicular fibers. It was also found that the loss factors do not decrease linearly with the volume fraction of aluminum. In addition, for a given volume percent of phases, the loss factors were found to be higher for coarse particles. This was attributed to the ability of the high damping phase to deform relatively independently. In addition to the loss factors, stress distributions were also determined and the stresses were found to be higher in Al which has higher Youngs modulus.

Introduction

Internal friction or damping is the ability of the material to absorb vibrational energy. In many applications, high damping is needed to reduce unwanted vibrations and acoustic noise. Composites are attractive for such applications because they can be designed suitably, by proper combination of phases. To optimize their damping behavior, it is necessary to understand the effects of various factors including volume fraction, size, shape, orientation and continuity of phases on overall damping of the composite. In this regard there is a lack of understanding. Analytical solutions available to date [1,2,3] are primarily concerned with specific morphologies and thus cannot predict the result of a change in the damping behavior with change in morphology of phases, even though they cannot account for volume percent changes. In this regard, the FEM seems to be a viable method for such studies [4-7]. Recently FEM has been successfully used to study the stress-strain [5,6] and damping behavior[7] of composites. The aim of this investigation was to systematically study the damping behavior of Epoxy/ Al composites by varying the size, volume fraction and morphology of the constituent phases with FEM.

When a harmonic stress is applied to a material, in the steady state, the corresponding strain lags behind the stress by an angle α. The stress-strain relationship can be expressed in complex form:

$$\sigma = E^* \varepsilon^* \quad \cdots\cdots(1)$$

where:

$$\sigma = \sigma_0 \exp[i(\omega t + \alpha)] \quad (2)$$

$$\varepsilon^* = \varepsilon_0 \exp(i\omega t) \quad (3)$$

with σ_0 and ε_0 being the amplitudes of the respective stress and strain cycles, and ω the angular frequency. The complex modulus is given by

$$E^* = E \exp(i\alpha), \text{ i.e., } E^* = E(\cos\alpha + i \sin\alpha) \quad (4)$$

where E is the absolute modulus which is equal to σ_o/ε_o. This can be written as

$$E^* = E' + iE'' \quad (5)$$

where

$$E' = E\cos\alpha \quad (6)$$

$$E'' = E\sin\alpha$$

i.e.,

$$E^* = E'(1+i\eta) \quad (7)$$

where η is the loss factor. The loss factor η is given by the ratio E''/E' which in turn is equal to $\tan\alpha$. Therefore, the phase lag between the stress and strain gives a measure of damping. Hashin[8] developed a theory to predict damping of reinforced composites from the properties of component phases.

$$\varphi_{11} = V_f(E_f/E_{11})\varphi_f + (1-V_f)(E_m/E_{11})\varphi_m \quad (8)$$

where V_f is the fiber volume fraction, E_{11} is the axial elastic modulus of the composite and $E_f, \varphi_f, E_m, \varphi_m$ are the elastic moduli and damping of the fiber and matrix, respectively. From Hashin [8], the complex longitudinal Youngs modulus of the composite in the fiber direction can be written as:

$$E^*_{compo} = V_f E^*_f + V_m E^*_m \quad (9)$$

where E^*_{compo} is the complex moduli of the composite, V_f and V_m are the volume fractions of the fiber and matrix, respectively, given by E^*_f and E^*_m are the complex moduli of the fiber and matrix respectively and where

$$E^*_f = E_f\cos\alpha_f + i\,E_f\sin\alpha_f \quad (10)$$

and

$$E^*_m = E_m\cos\alpha_m + i\,E_m\sin\alpha_m \quad (11)$$

Substituting equations 10 and 11 in equation 9, we get:

$$E^*_{compo} = (V_f E_f\cos\alpha_f + V_m E_m\cos\alpha_m) + i\,(V_f E_f\sin\alpha_f + V_m E_m\sin\alpha_m) \quad (12)$$

From the above equation, the loss factor for the composite can be

Advanced Composites '93
International Conference on Advanced Composite Materials
Edited by T. Chandra and A.K. Dhingra
The Minerals, Metals & Materials Society, 1993

written as:

$$\tan \alpha = \text{Imag } (E^*_{compo}) / \text{Real } (E^*_{compo}) \qquad (13)$$

which from equation 12 can be derived to be:

$$\tan \alpha = (V_f E_f \sin\alpha_f + V_m E_m \sin\alpha_m) + (V_f E_f \cos\alpha_f + V_m E_m \cos\alpha_m) \qquad (14)$$

Equation 14 is used to calculate loss factors for a composite with parallel fibers and these are compared with loss factors computed using FEM.

Procedure

The NASTRAN computer program [10] which is based on FEM principles was used in the present investigation. NASTRAN rigid format number 9, Direct Transient Response Analysis, was used to predict the damping behavior of the composites. This solution sequence of NASTRAN uses the following force balance equation:

(Inertial Forces) + (Viscous Forces) + (Spring Forces) = (Applied Force)

The inertial forces are given by mass times the acceleration, Mx, the viscous forces are given by Bx where B is the viscous damping coefficient and the spring forces are given by Kx where K is the stiffness. The above equation can be written as:

$$Mx + Bx + Kx = F \qquad (15)$$

This equation can be written as follows using the derivative operator:

$$[Mp^2 + Bp + Kp](x) = [F] \qquad (16)$$

where [M] is the Mass matrix, [B] is the damping matrix, [K] is the stiffness, (x) is the vector of displacements, [F] is the vector of the applied forces, and p = d/dt. The load is applied in the form of:

$$F = A \sin(2\pi ft) \qquad (17)$$

where A = 0.75 lbs (0.341 Kgs)., f= 1 Hz.

The FEM procedure employed in this kind of investigation is similar to that used earlier [7]. To study the effect of morphology, i.e., to compare fibers with particles, several FEM meshes were prepared with 25, 50 and 75 % vol. of aluminum and load was applied in plane as shown in Figs. 1 and 2. A typical mesh with 50 volume % fibers parallel to the loading direction is shown in Fig. 1 and another mesh with perpendicular fibers is shown in Fig. 2. Meshes with fine particles (size corresponding to those shown in Fig. 3, but under in plane loading conditions) were also prepared but they are not shown here. In plane loading was used primarily to compare the FEM calculated results and Hashins theory for the parallel fibers where the agreement was found to be excellent.

To predict particle size effects, FEM meshes with different volume % aluminum were made with three different particle sizes for each volume fraction. A typical mesh corresponding to fine particle sizes of aluminum (or epoxy) with 50 volume % of each phase is shown in Fig.3. The corresponding mesh with coarse particles is shown in Fig. 4. It is to be noted that for the particle size effect study, the load was applied perpendicular to the plate as shown in Figures 3 and 4. This loading was selected because this is how experimental work is normally carried out by various investigators to measure the damping of composites. In addition to calculating the loss factors of various composites, stress distributions and the corresponding displacements along a given section, such as that denoted as 1-1' in Fig. 3, were also calculated.

Results and Discussion

The loss factors calculated for the perpendicular and parallel fibers and for fine particles where the load was applied in the plane of the plate, as shown in Fig. 1, are shown in Fig. 5. It is to be noted that the loss factors obtained for parallel fibers are very close to those obtained by Hashin's theory [8,9]. This close correspondence appears to be related to the fact that the assumptions made in both the analyses are similar. This close correspondence also confirms the accuracy of the FEM method employed in this investigation. Observation of Fig. 5 indicates that the damping behavior of composite materials cannot be predicted by the simple law of mixtures. For a given volume fraction of phases, the

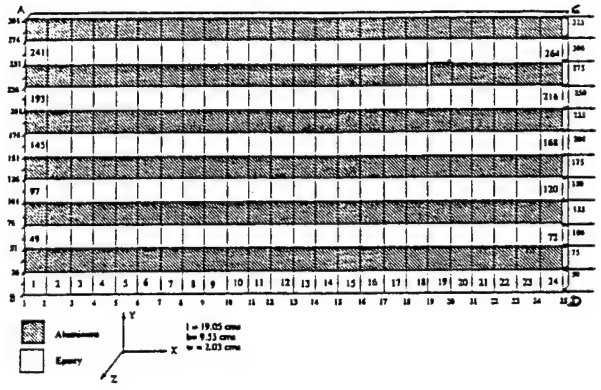

Fig. 1 : FEM mesh used to calculate loss factor of epoxy-50 vol.% Al composite, with aluminum fibers parallel to in-plane loading direction

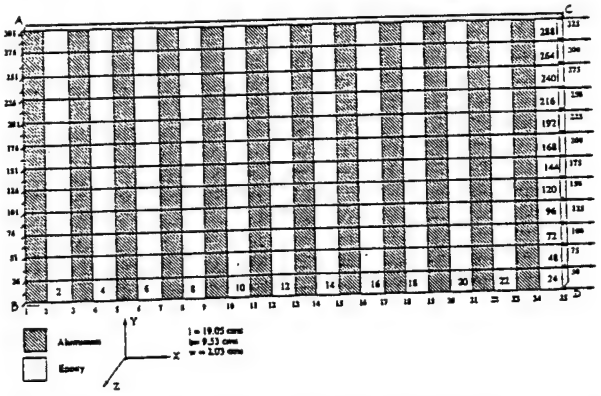

fig. 2 : FEM mesh used to calculate loss factor of epoxy-50 vol.% Al composite, with aluminum fibers perpendicular to in-plane loading direction

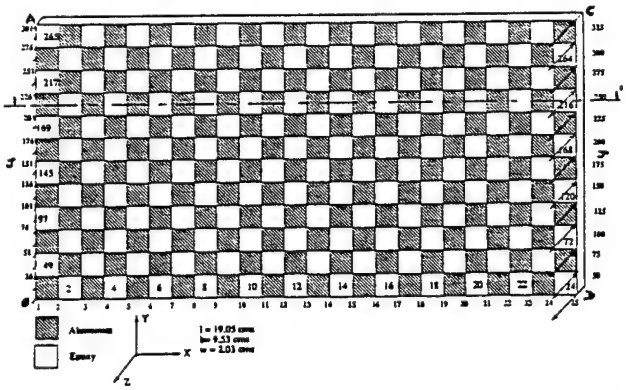

Fig. 3 : FEM mesh used to determine the loss factor of epoxy-50 vol.% Al composite, with fine aluminum particles

damping of the composite with parallel fibers is much lower than that of perpendicular fibers. This appears to be related to the fact that in the former case the component phases are constrained to undergo the same amount of deformation in the direction of loading. This constraint comes from the way the composite is pulled or deformed. Because of the constraint, the phase with high damping is not free to damp to the extent it can under a given load. However, in the case of perpendicular fibers, i.e., when the fibers are perpendicular to the loading direction, the situation is different. Here, for a given loading condition, the component phases can deform relatively freely and hence can damp relatively freely resulting in higher overall damping of the composite. It is extremely important to note that this does not mean that the damping of composites may be calculated by the law of mixture rule using the

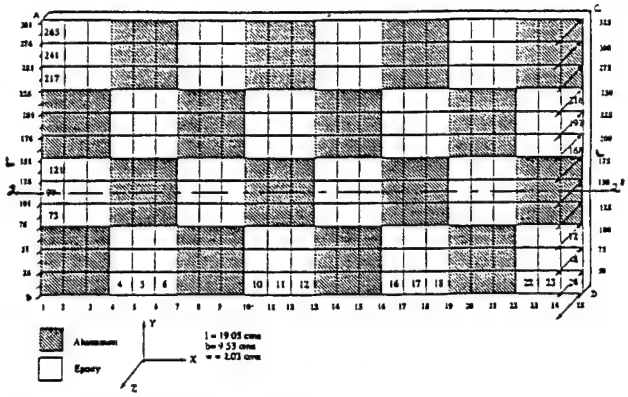

Fig. 4 : FEM mesh used to determine the loss factor of epoxy-50 vol.% Al composite, with coarse aluminum particles

constant stress assumption [12,13]. As Fig. 5 clearly indicates, the loss factors calculated using the correspondence principle and constant stress assumption are much higher than those calculated using law of mixture. The loss factors of composites with fine particles are in between those of perpendicular and parallel fibers. This is due to the fact that the constraints for this condition are less severe than those for parallel fibers and more severe than those for perpendicular fibers.

The loss factors corresponding to the study on particle size effects with perpendicular loading are shown in Fig.6. The relative particle sizes are indicated at the bottom of this figure. For a given volume fraction, as the particle size decreases, the interface area for unit volume increases and so also the constraints. This in turn results in lower damping because the high damping component phase cannot damp/deform relatively freely. As shown in Fig. 6, the

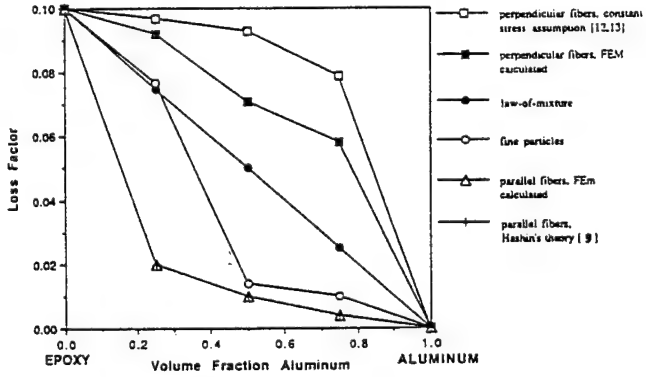

Fig. 5 : Loss factor versus Aluminum content for Epoxy-Aluminum composites

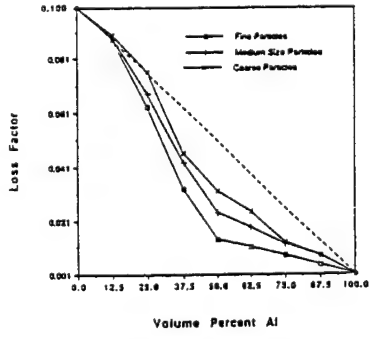

Fig. 6 : Effect of volume percent of aluminum on the loss factors of the epoxy-aluminmum composites

damping of the composite decreases with decrease in particle size. This trend is true for all of the volume fractions of aluminum considered in this investigation.

As mentioned earlier, in addition to calculating the loss factors, the stress distributions and displacements were also studied. Stress distributions along section 1-1' of Fig. 3 are shown in Fig. 7. As expected, the stresses were found to be non-uniform. The stresses were higher in aluminum which has a higher modulus than in epoxy. It is to be noted that most of the analytical solutions cannot predict such stress distributions which are of importance in understanding the failure behavior of composites under dynamic loading conditions.

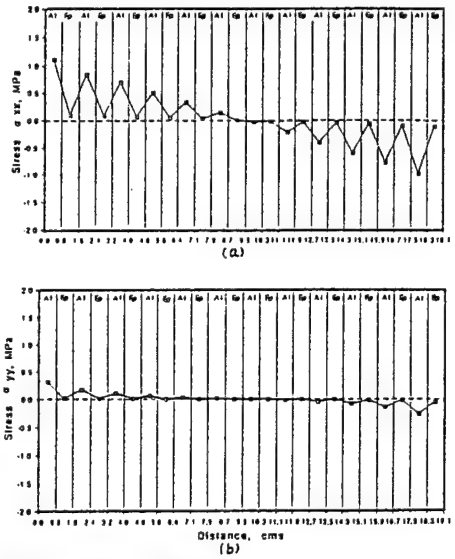

Fig. 7 : Transverse stresses along section 1-1' of Fig. 3 : (a) σ_{xx} , (b) σ_{yy}

Conclusions

1. A two dimensional FEM method was employed to determine the damping behavior of various Epoxy-Al composites, with different volume percents and morphologies of phases. The quantities determined included loss factors, stress distributions and displacements.
2. The loss factors of composites with Al or Epoxy fibers perpendicular to the loading direction were found to be much higher than those for parallel fibers. This was attributed to the constrained deformation in the latter case. The loss factors of the composites with fine particles of Al or Epoxy were found to be in between those of parallel and perpendicular fibers. This was attributed to the fact that the particles are neither completely free nor completely constrained to undergo independent deformation.
3. It was found that the loss factors do not decrease linearly with the volume percent of the second phase. For particulate composites, the loss factors are much lower than what one would expect by the law of mixtures. The actual decrease depended on particle size of the phases.
4. For a given volume percent of phases, the loss factors with coarse particles were found to be higher. This was attributed to the ability of the high damping phase to damp relatively independently at regions inside the phase.
5. In general, at any given time, the stresses in the stiffer Al phase were found to be higher. This was attributed to the constrained deformation of the commonly shared interfaces, resulting in higher stresses in Al.

Acknowledgements

This project is being funded in part by the David Taylor

Research Center and the Office of Naval Research under grant number N 00014-92-J-4039. The authors wish to express their appreciation to Dr. Larry Kabacoff of the Office of Naval Research and Mr. Ivan Caplan of CD/NSWC for their encouragement and support. The authors would like to thank the Computer Science Center of the University of Maryland for the computer time.

References

1. M.L.Soni and F.K.Bogner, AIAA Journal,11982, p.700.
2. C.D.Johnson and D.A.Keinholzz, AIAA Journal, 20, 11982, p.1284.
3. S.J.Huang and R.F.Gibson, J.Eng.Mat.Tech., ASME, 109, 1987, p.47.
4. S.Ankem and H.Margolin, Metall. Trans., 13A, 11982, p. 603.
5. S.Neti, M.N.Vijayshanker and S.Ankem, Mats.Sc. &Eng., A145, 1991, p.47.
6. S.Neti, M.N.Vijayshanker and S.Ankem, Mats.Sc. & Eng., A145,1991,p.55.
7. S.Neti, A.Nanavaty,S.Ankem and C. Wong,Proceedings of the M^3D Conference on Material Damping, Baltimore, MD, March 1991.
8. Z.Hashin, Int. J. Solids and Struct., 6(5),1970, p. 539.
9. Z.Hashin, Int. J. Solids and Struct., 6(6),1970, p. 797.
10. NASTRAN Users Manual Level 17.5, Sept. 1983, Document NASA SP-222(06), Published by National Aeronautics and Space Administration, Washington DC.
11. G.G.Wren and V.K.Kinra, Journal of Testing and Evaluation, JTEVA, 16, 1988, p. 77.
12. S. Ankem and K.S.Kannan, Unpublished Research, University of Maryland, 1992.
13. K.S.Kannan and S.Ankem, Proceedings of the Symposium," Damping of Multiphase Inorganic Materials," Nov. 1-5, Chicago, 1992.

2C. TECHNICAL PROGRESS : PART III

The Effect of Volume Percent and Morphology of Phases on the Damping Behavior of Epoxy/Aluminum Composites

JYOTHI G. RAO and SREERAMAMURTHY ANKEM

In this investigation, the finite element method (FEM) has been employed to predict the effects of volume percent and morphology, including size, shape, and continuity of phases, on damping behavior of epoxy/Al composites. It is shown that for a given volume percent of phases, the loss factor of the composite increases with an increase in particle size. The effect of matricity was obtained by selecting a composite with 50 vol pct of each phase and arranging, in one case, aluminum as the particle phase and, in the other case, aluminum as the matrix phase. The loss factor obtained for the former was found to be much higher. This was attributed to the ability of the epoxy phase when it is in the form of matrix to damp/deform relatively freely. The normal stress distributions and two-dimensional (2-D) hydrostatic stress distributions were also predicted. In general, the stresses were found to be higher in the stiffer aluminum phase and the stress gradients were found to increase with an increase in particle size for a given volume percent of phases. The 2-D hydrostatic stresses were also found to be higher in the stiffer aluminum phase and the stress gradients were found to increase with an increase in particle size as well.

I. INTRODUCTION

THE damping capacity of a material is the ability of the material to dissipate vibrations by converting the vibrational energy into other forms of energy. In metallic systems, this energy dissipation occurs by the release of heat, which is caused by internal friction across the specimen. Polymeric materials have high damping capacity, usually more than an order of magnitude greater than structural metallic materials, but in general, they have low stiffness.

Composites are a class of materials whose properties can be tailored according to specific requirements by varying the component phases. For many applications, the goal is to obtain high damping with reasonable stiffness. In composite materials, there are numerous methods of energy dissipation, such as by viscoelastic response of the material constituents in polymer systems, thermoelastic conversion of mechanical energy into heat, friction at the fiber-matrix or particulate-matrix interface, and from the absorption of vibrational energy during microplastic deformation of the particle itself. The nonhomogeneous characteristics of the composite give rise to damping due to the resulting stress variations across the interfaces. The problem of low stiffness can be overcome by reinforcing polymers with rigid particulates or fibers resulting in optimal damping and stiffness.

The present study involves the damping behavior of fiber and particulate epoxy/Al composites. The damping behavior of such a composite depends on complex interplay between the properties of the individual constituent phases: the resin, the filler, and the interfacial phase. The loss factor of a composite is affected by a number of parameters, such as size, shape, aspect ratio, distribution, adhesion between phases, and continuity of the phases. Most of the analytical solutions available are concerned with specific geometries and are not suitable to predict the damping behavior of composites as a function of these morphological factors. In this study, the finite element method (FEM) has been employed to study the damping behavior of the epoxy/Al composites as a function of particle size, morphology, and volume percent of the phases.

II. TECHNICAL BACKGROUND

Damping capacity of a material can be measured/characterized in a number of ways. Damping is measured either during free decay or during continuous driving force, at a given frequency and strain amplitude. The simplest experiment to measure damping involves a cantilever beam which is excited or loaded into its fundamental mode of vibration by an external force. The damping capacity can be measured in a number of ways, one of which is loss factor. This is described subsequently.

The modulus of a viscoelastic material is expressed as a complex quantity. When a harmonic stress is applied to a material in steady state, the corresponding strain lags behind the applied stress by an angle ϕ. The loss factor is given by the tangent of the phase angle, ϕ, between stress and strain. The stress-strain relationship can be expressed in a complex form as

$$\sigma^* = E^*\varepsilon^* \quad [1]$$

where

$$\sigma^* = \sigma_0 \exp [i(\omega t + \phi)] \quad [2]$$

and

$$\varepsilon^* = \varepsilon_0 \exp (i\omega t) \quad [3]$$

with σ_0 and ε_0 being the amplitudes of the respective stress

JYOTHI G. RAO, Graduate Student, and SREERAMAMURTHY ANKEM, Associate Professor, are with the Department of Materials and Nuclear Engineering, University of Maryland, College Park, MD 20742-2115.

This article is based on a presentation given in the Mechanics and Mechanisms of Material Damping Symposium, October 1993, in Pittsburgh, Pennsylvania, under the auspices of the SMD Physical Metallurgy Committee.

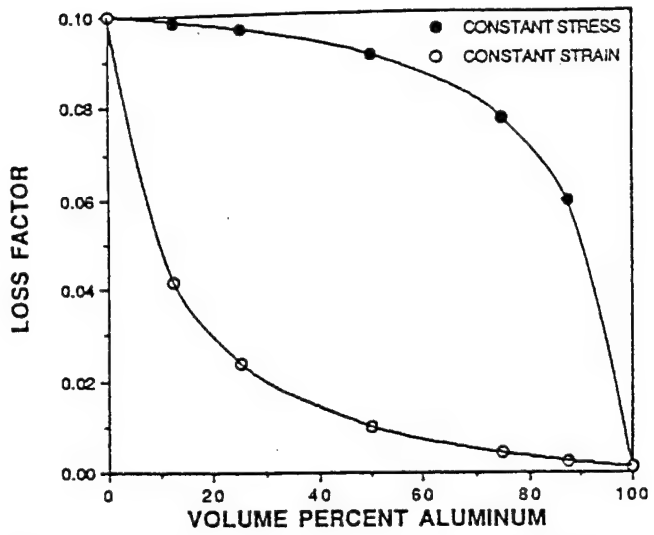

Fig. 1—Comparison of loss factors of epoxy/Al composites obtained by using the analytical equations based on the assumptions of constant strain, parallel fibers and constant stress, perpendicular fibers.

and strain cycles and ω the angular frequency. The complex modulus is

$$E^* = E \exp(i\phi) \quad [4]$$

or

$$E^* = E' + iE'' \quad [5]$$

where E' is the storage modulus representing strain energy and E'' the loss modulus representing the energy dissipated in the material. The loss factor η can be derived from the preceding equation, is given by the ratio of E''/E', and is equal to $\tan\phi$. Therefore, the phase lag between the stress and strain gives a measure of damping.

There are a number of analytical solutions available for specific geometries, *e.g.*, for the Voigt structures, where the continuous fibers are parallel to the loading direction. Hashin[1,2] obtained the loss factor of the composite with Voigt structure in terms of the loss factors of the individual phases. The solution is as follows:

$$\eta = \frac{V_f E_f \sin\Phi_f + V_m E_m \sin\Phi_m}{V_f E_f \cos\Phi_f + V_m E_m \cos\Phi_m} \quad [6]$$

where V_f and E_f are the volume fraction and elastic modulus of fibers, respectively, and V_m and E_m are the volume fraction and elastic modulus of the matrix, respectively. Similarly, for the Reuss structure, where the continuous fibers are perpendicular to the loading direction, and with the correspondence principle, the loss factors of the composite have been obtained, and this relation is shown:[3,4]

$$\eta = \frac{\eta_1 V_1 E_2 + \eta_2 V_2 E_1 + \eta_1^2 \eta_2 V_2 E_1 + \eta_2^2 \eta_1 V_1 E_2}{V_2 E_1 + V_1 E_2 + \eta_1^2 V_2 E_1 + \eta_2^2 V_1 E_2} \quad [7]$$

where η_1, V_1, and E_1 are loss factor, volume fraction, and elastic modulus of phase 1 and η_2, V_2, and E_2 are loss factor, volume fraction, and elastic modulus of phase 2. From these two equations, the loss factors of the epoxy/Al composites with continuous fibers have been calculated and are shown in Figure 1. It can be seen that for a given volume percent, the loss factor of the composite with Voigt structure is much lower than the Reuss structure. To a first approximation, these two curves can be treated as the lower bound, constant strain and upper bound, constant stress, respectively. In addition, a number of analytical solutions are available[5] for very specific geometries. However, most of the solutions cannot predict the change in the loss factor of a given composite as a function of the morphology of the phases, such as particle size, distribution, and continuity of phases. In this regard, the FEM method appears to be very effective[3,6] and has been used in the present study. In addition to predicting the loss factor of the composite, FEM can also predict the local stress distributions. The FEM procedure employed in this investigation is described in Section III.

III. DESCRIPTION OF FEM PROCEDURE

As mentioned previously, the FEM method has been used to predict the damping behavior of epoxy/Al composites as a function of volume fraction and morphology of the phases. The ANSYS computer program,[7] which is based on FEM principles, has been employed.

The direct harmonic response analysis was used to predict the damping behavior of the composite. The time-dependent equations of motion for linear structures undergoing steady-state vibration are solved to obtain the damping matrix and subsequently the loss factor. The following assumptions and restrictions are imposed on the analyses:

(1) the entire structure has constant stiffness, damping, and mass effects; and
(2) all loads and displacements vary sinusoidally at the same known frequency but might not be necessarily in phase.

The following force balance equation is used for the calculations:

(inertial forces) + (viscous forces) + (spring forces) = (applied forces)

The preceding equation can be written as

$$[M]\{\ddot{\mathbf{u}}\} + [C]\{\dot{\mathbf{u}}\} + [K]\{\mathbf{u}\} = \{\mathbf{F}\} \quad [8]$$

where $[M]$, $[C]$, and $[K]$ are the mass, damping, and stiffness matrices of the structure, respectively; $\{\ddot{\mathbf{u}}\}$, $\{\dot{\mathbf{u}}\}$, and $\{\mathbf{u}\}$ are the vectors of nodal acceleration, velocity, and displacement, respectively; and $\{\mathbf{F}\}$ is the vector of external loads.

For FEM modeling, a plane stress cantilever type beam geometry has been assumed. Figure 2 is a representative FEM mesh used for the present study of epoxy/Al composites. The edge BC is clamped, and before the load is applied, the nodes at the edge BC have zero displacement. The entire beam is divided into a number of elements, and each element has four nodes. The force is applied to the right edge BC, and the nodes on the edge BC are constrained in such a way that all of them are forced to deform to the same extent. The darker elements represent Al, and the lighter elements represent the epoxy. The material properties for Al and epoxy are given in Table I. The length, breadth, and thickness of the beams were 0.19, 0.095, and 0.0203 m, respectively. A load of 40.08 N was applied along the x direction for all of the meshes at a vibration frequency of 1 Hz.

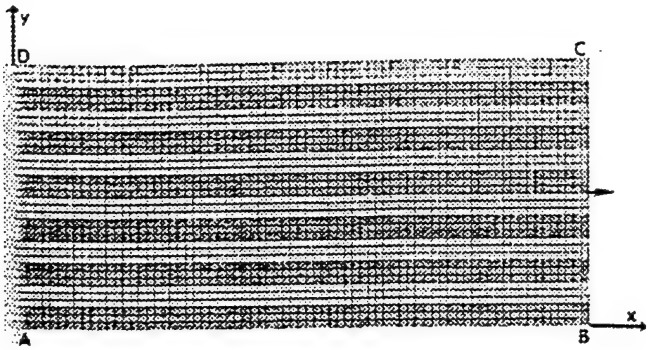

(*a*)

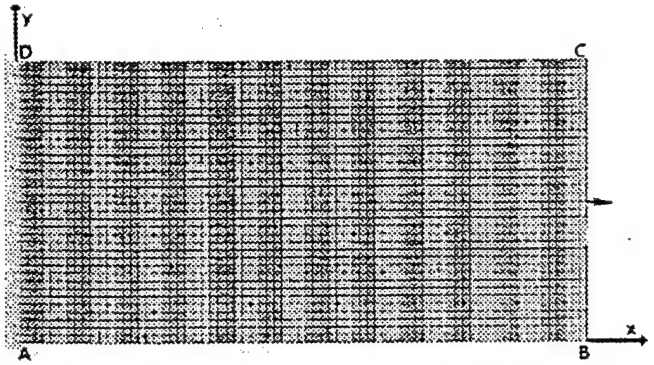

(*b*)

Fig. 2—FEM meshes with 50 vol pct of epoxy and 50 vol pct of aluminum composite: (*a*) parallel fibers and (*b*) perpendicular fibers. The lighter phase is epoxy, and the darker phase is aluminum.

Table I. Input Parameters of Aluminum and Epoxy

Material	Elastic Modulus (Pa)	Loss Factor	Density (Kg/m³)	Poisson's Ratio
Aluminum	6.9×10^{10}	0.001	2700.0	0.34
Epoxy	6.9×10^{9}	0.100	1194.2	0.34

The necessary constraints should be specified so that the program can recognize the nodes with the different degrees of freedom and accordingly arrange them into the master and slave nodes. In the ANSYS program, Eq. [8] is solved by means of Gaussian elimination and the Guyan method to obtain the damping matrix. Various meshes were prepared corresponding to the different volume percents of the phases, particle size, shape, and continuity of the phases. Some of the meshes used are shown in Figures 2 through 5.

The volume percent of the aluminum was varied from 12.5 to 87.5, with an increment of 12.5 pct of aluminum. The meshes corresponding to 50 vol pct of aluminum in the form of continuous fibers are shown in Figure 2. Figure 2(a) corresponds to the Voigt structure, and Figure 2(b) corresponds to the Reuss structure. The other meshes corresponding to 25 and 75 of aluminum for both of these configurations were also carried out but are not shown here.

The shape effect is studied by keeping the second phase in the form of particles, as shown in Figure 3. The meshes in Figure 3(a) through (c) correspond to 12.5, 50, and 87.5 vol pct aluminum, respectively. Calculations were also performed with other volume percents of aluminum but are

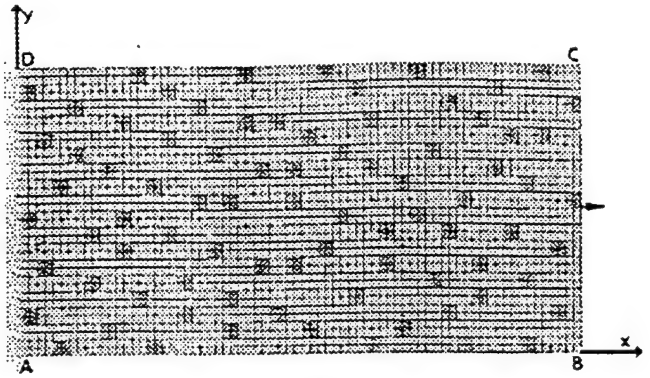

(*a*)

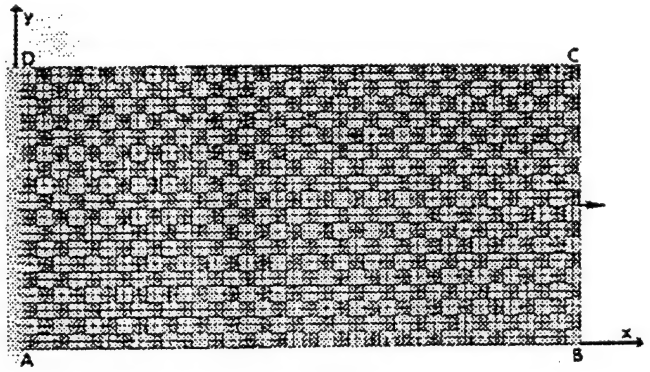

(*b*)

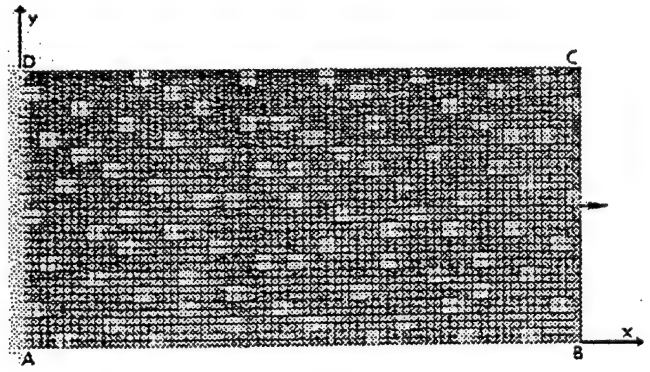

(*c*)

Fig. 3—FEM meshes with different amounts of second-phase particles: (*a*) 12.5 vol pct of aluminum particles in the epoxy matrix, (*b*) 50 vol pct of aluminum and 50 vol pct of epoxy particles, and (*c*) 12.5 vol pct of epoxy particles in the aluminum matrix. Note each particle has four elements.

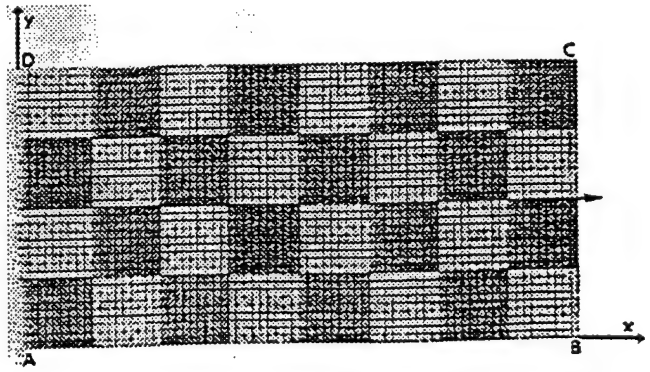

Fig. 4—FEM mesh consisting of medium-sized particles, 81 elements per particle, with 50 vol pct of each phase.

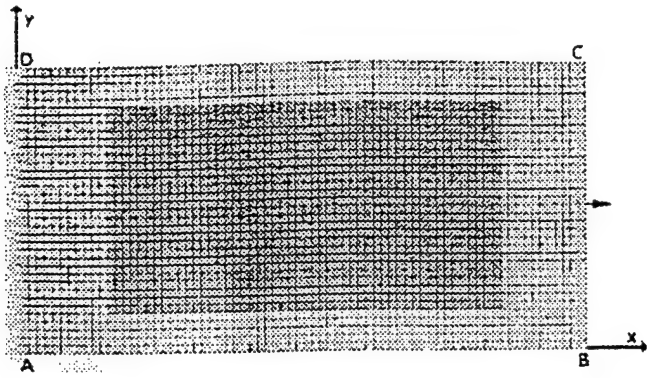

(*a*)

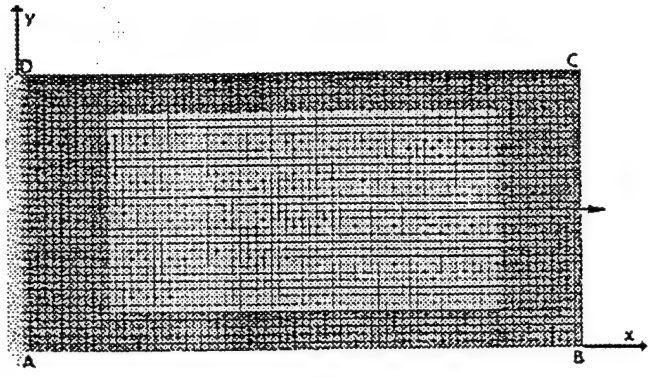

(*b*)

Fig. 5—FEM meshes used to determine the effect of continuity of phases: (*a*) 50 vol pct aluminum particle in the epoxy matrix and (*b*) 50 vol pct epoxy particle in the aluminum matrix.

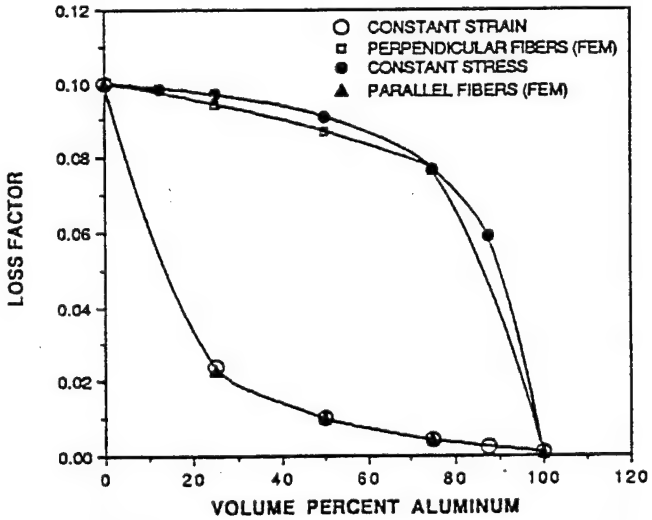

Fig. 6—Comparison of loss factors of epoxy/Al composites with continuous fibers obtained by analytical solutions based on the constant strain and constant stress assumptions with those obtained by FEM.

not shown here. It should be noted that when aluminum is less than 50 vol pct, it is in the form of particles, and when it is greater than 50 vol pct, it is in the form of the matrix.

The particle size effect was studied by varying the relative particle size to be 18 times that of the smallest size. The size of the particles is increased by increasing the number of elements within a particle (note: element size is fixed for all particle sizes). The smallest particle contains one element per particle (not shown here), and the largest particle contains 324 elements per particle (also not shown here). Figure 4 shows the mesh for a medium-sized particl with 81 elements in each particle, where the aluminum content is 50 vol pct. The meshes corresponding to other intermediate sizes and volume percents are not shown here to minimize the number of figures.

To study the effect of matricity for a given volume percent of the phases, in one case, epoxy was made as the continuous phase and, in the other case, the aluminum was made as the continuous phase. The meshes corresponding to 50 vol pct of aluminum particle and 50 vol pct of epoxy particle are shown in Figures 5(a) and (b), respectively.

Based on the material properties for epoxy and aluminum, including elastic constants, loss factors, and the constraints imposed, the ANSYS program calculates the overall loss factor of the composite and the longitudinal and transverse stresses. In addition to studying the loss factors and normal stress distributions, two-dimensional (2-D) hydrostatic stress distributions were calculated and studied.

IV. RESULTS AND DISCUSSION

To check the accuracy and reproducibility of the FEM procedure employed, meshes similar to Figure 2(a) were made, except that all the elements were made up of only aluminum in one case and only epoxy in the other case and the loss factors were determined. The loss factors obtained were found to be extremely close to the input loss factor of aluminum and epoxy, respectively. This suggested that the FEM procedure employed is very accurate and reproducible. Then, calculations were performed with various meshes of epoxy/Al composites, and the effects of volume percent, particle shape, size, and matricity were determined. The results obtained include the loss factors of the composite, displacements, normal and transverse stress distributions, and hydrostatic stress distributions (2-D). Loss factors, normal stress distributions, σ_x, and hydrostatic stress distributions, *i.e.*, $(\sigma_x + \sigma_y)/2$, are presented separately in the following sections. The transverse stress distributions, σ_y, are not presented here.

A. *Loss Factors*

1. *Comparison of FEM results with analytical solutions*

The loss factors obtained by FEM for parallel and perpendicular fibers are compared with those obtained by analytical solutions in Figure 6. It should be noted that the loss factors obtained by analytical solutions by constant strain assumption and those obtained by FEM for parallel fibers exactly coincide. This is expected because the constant strain assumption made in the analytical solution is also followed in the FEM procedure by the way the composite is stressed (Figure 2(a)) and the way constraints are imposed on the edge BC. However, for perpendicular fibers (Figure 2(b)), the assumption made in the analytical solutions, *i.e.*, constant stress, is not strictly correct because of the end effects on edges AB and CD. Therefore, slight deviations were found and the loss factors obtained by FEM are more accurate. Nevertheless, the loss factors obtained by the analytical solutions based on constant strain and constant stress assumptions can be treated, to a first approxi-

mation, as the lower bound and the upper bound, respectively. It should be noted that this is in reverse to the bounds of the elastic moduli obtained on the basis of constant strain and constant stress assumptions.

2. *Effect of orientation of fibers*

Observation of Figure 6 shows that for a given volume percent of phases, the loss factor of the composite with continuous fibers, where the fibers are oriented parallel to the loading direction, is much lower than that where the fibers are oriented perpendicular to the loading direction. This difference is related to the constrained deformation in the case of the parallel fibers (Figure 2(a)). In this case, the composite is deformed in such a way that both the phases must deform to the same extent at any given stage of deformation. This means that the high damping phase cannot damp/deform independently, and this results in lower damping of the composite. In the case of the perpendicular fibers (Figure 2(b)), the phases are relatively free to damp/deform giving rise to high damping. There is considerable experimental evidence in the literature to support these results. For example, Wren and Kinra[8] and Crane and Gillespie[9] have shown that the damping of the composite with continuous fibers parallel to the loading direction is much lower than that of the composite with perpendicular fibers.

3. *Effect of shape and size*

The loss factors obtained by FEM with various particle sizes of epoxy/Al composites are shown in Figure 7. It should be noted that the smallest particles have one element in each particle and the largest particles have 324 elements in each particle, as indicated in Figure 7. This figure shows that the loss factor of a given composite is greater when the second phase is in the form of particles as compared to parallel fibers. This is due to the fact that the continuous fiber-reinforced composites, when loaded in the longitudinal direction of fibers, must undergo constrained deformation. In the case of composites with particles, the constraints are primarily limited to the areas near the interphase interfaces. Therefore, the high damping phase in the case of the particulate composite is relatively free to damp/deform independently. This gives rise to higher damping of the composite. These findings are consistent with the experimental results of Zhang *et al.*[10] and Rohatgi *et al.*,[11] who reported higher damping for particulate-reinforced metal matrix composites as compared to the continuous fiber-reinforced metal matrix composites.

For a given volume percent of phases, Figures 7(a) and (b) indicate that the loss factor of epoxy/Al composites increases with the increase in particle size of the second phase. This is related to the interphase interface areas and the ability of the second phase to deform freely. As particle size increases, the interphase interface area per unit volume decreases (*e.g.*, compare Figures 3(b) and 4). This means that the interfacial area at which the two phases must undergo the same extent of deformation decreases with an increase in particle size. The net effect is a decrease in constraints imposed on each other, *i.e.*, the high damping phase can damp/deform relatively freely with increasing particle size, and this results in higher damping. There is considerable experimental evidence to support these results. For example, Adams and Fox[12] found that in the cast iron/graphite composite, the damping capacity of the composite increases with an increase in graphite flake size.

4. *Effect of volume fraction and matricity*

The three-dimensional (3-D) plot shown in Figure 7(c) shows the effect of particle size and volume fraction on the loss factor of various epoxy/Al composites. It should be noted that, here, particle size refers to the minor phase in the composite. When the aluminum is less than 50 vol pct, epoxy is the matrix phase. The addition of Al to epoxy decreases the loss factors, and the extent of decrease depends on the size of Al particles. The rate of decrease is lower for composites with larger sizes. This is due to the constraints outlined earlier. In the case of a composite with greater than 50 vol pct Al, the addition of epoxy increases the loss factor of Al. The increase depends on the epoxy particle size. Observation of Figures 7(a) and (c) indicates that a drastic change occurs when the addition of epoxy to Al is greater than 50 pct. Conversely, the decease in damping with Al addition beyond 50 vol pct is much less. This is due to the change in matricity, the effect of which is described subsequently.

As the amount of Al increases beyond 50 vol pct, the matrix changes from epoxy to Al; *i.e.*, when Al is less than 50 vol pct, epoxy is the matrix phase, and when epoxy is less than 50 vol pct, Al is the matrix phase. To study the effect of matricity, two meshes (Figures 5(a) and (b)) were prepared, and the loss factor predicted by FEM is shown in Figure 8. For comparison purposes, the loss factors obtained by constant stress and constant strain assumptions are also included. When the high damping but lower stiffness epoxy phase is the matrix, the loss factor is much higher. This is due to the fact that the epoxy phase can deform/damp relatively freely, giving rise to high damping. The damping so obtained is close to the damping obtained analytically by constant stress assumption. On the other hand, when epoxy is in the form of particles embedded inside the stiffer but low damping alumina phase, the epoxy cannot damp/deform relatively freely, thereby giving rise to lower damping of the composite. This is the reason why sharp changes occur in the loss factor *vs* volume percent of Al plot (Figure 7(a)) around 50 vol pct, particularly for the composite with small particles.

B. *Normal Stress Distribution*

Normal stress distributions, σ_x, are obtained corresponding to meshes shown in Figures 2(a) and (b). Those distributions are not shown here, but they reveal that the stresses corresponding to Figure 2(a) are much higher in the stiffer aluminum as compared to the epoxy. This is due to the fact that both phases must undergo the same amount of deformation because of constraints imposed on edge BC. On the other hand, stress distributions corresponding to Figure 2(b) were found to be quite uniform, *i.e.*, similar stresses in both aluminum and epoxy except near the edges AB and CD. The uniform stress distributions for mesh, shown in Figure 2(b), suggest that the constant stress assumption for such a configuration is quite reasonable.

Normal stress distributions were also obtained for various meshes corresponding to different particle sizes and volume fractions. For illustration, the normal stress distri-

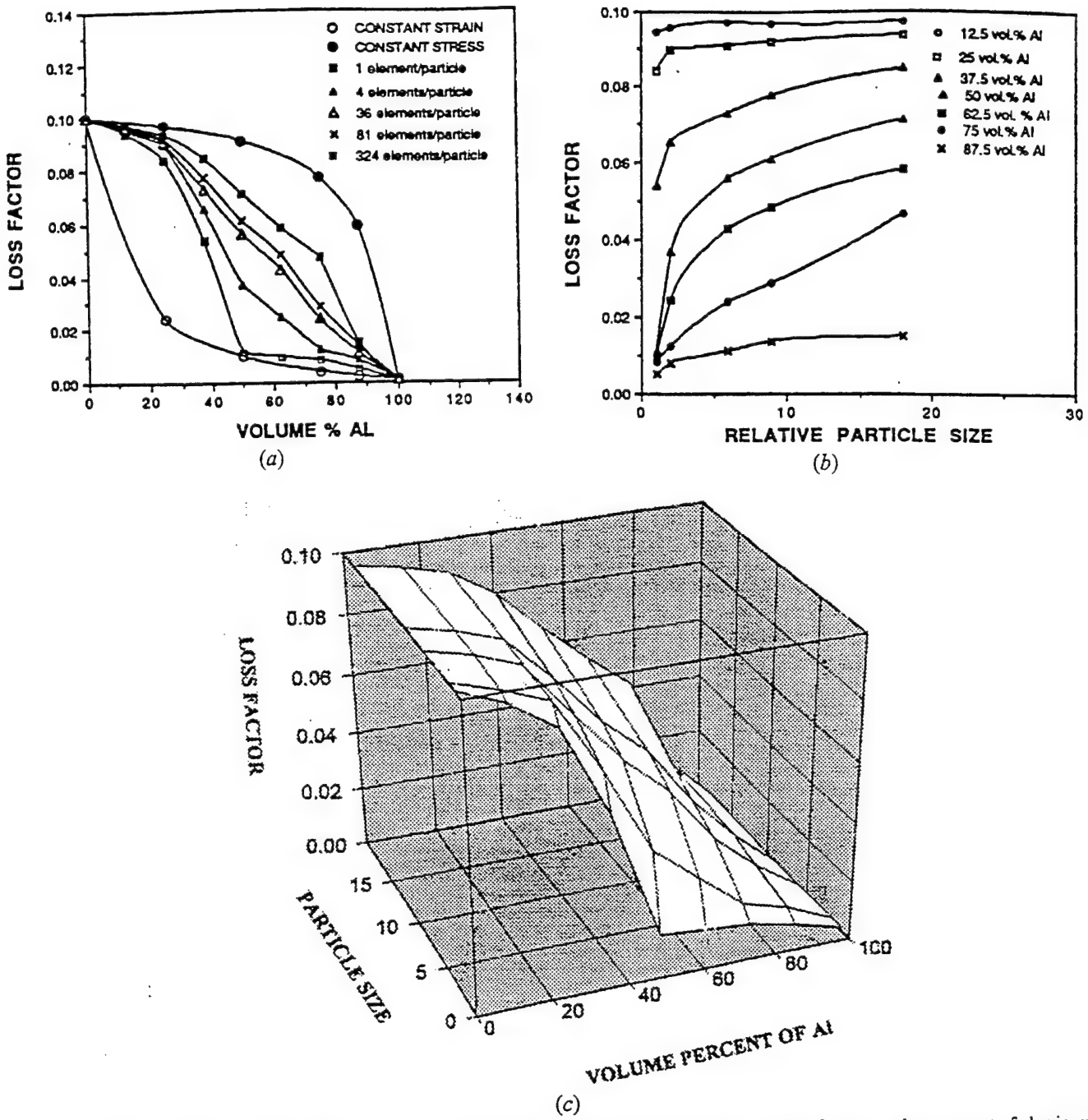

Fig. 7—The effect of particle size and volume percent on the loss factor of the epoxy/Al composites: (*a*) loss factor *vs* volume percent of aluminum for different particle sizes (loss factors obtained by analytical solutions are also included for comparison), (*b*) loss factor *vs* particle size for different volume percents of aluminum, and (*c*) a 3-D plot with loss factor, particle size, and volume percent of aluminum as the parameters.

butions corresponding to Figures 3(a) and (c) are shown in Figures 9(a) and (b), respectively. These figures reveal that the stresses are nonuniform for both cases, whether aluminum phase is in the form of particles (Figure 3(a)) or aluminum is in the form of the matrix (Figure 3(c)). In both cases, the stresses are higher in the stiffer aluminum phase and lower in the epoxy phase (Figures 9(a) and (b)). Similar observations were also made for other volume percents of phases and particle sizes. For a given volume percent, the stress distributions showed an increase in stress gradients with an increase in particle size. This is related to the ability of the component phases to deform relatively independently at regions far away from the interphase interfaces in the case of coarse particles.

C. *Hydrostatic Stress Distributions*

To determine the probable sites for void or crack formation, 2-D hydrostatic stresses, $(\sigma_x + \sigma_y)/2$, are obtained for various volume percents and morphologies. For illustration, the hydrostatic stress distributions corresponding to meshes in Figures 3(b) and 4 are shown in Figure 10(a) and (b), respectively. The hydrostatic stress distribution in Figure 10(a) shows larger stresses in aluminum than in ep-

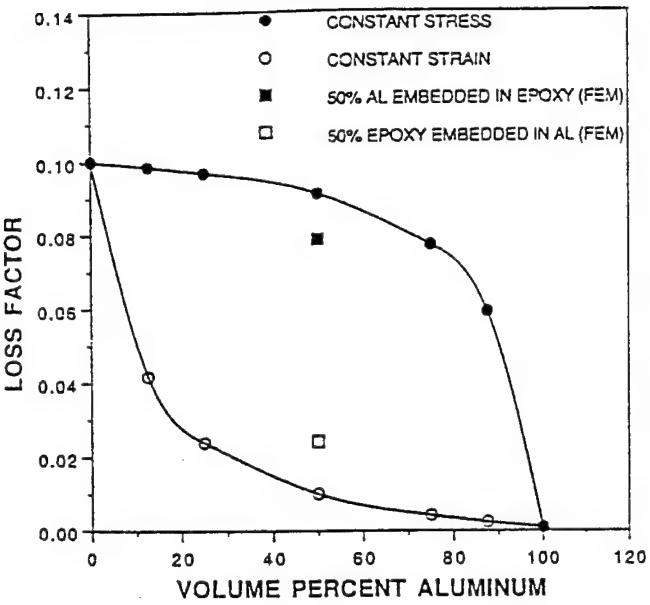

Fig. 8—The effect of matricity on the loss factors of epoxy/Al composites. Analytical loss factors are also included for comparison.

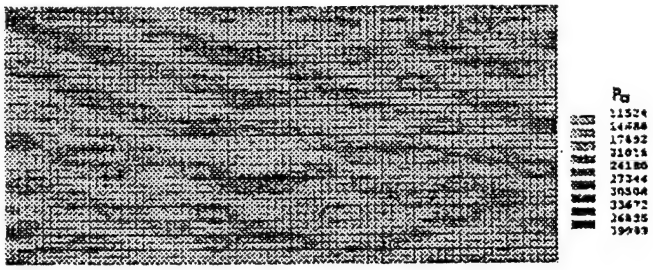

(*a*)

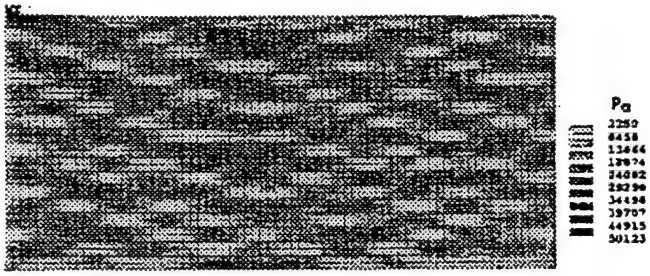

(*b*)

Fig. 9—The effect of volume percent on the normal stresses distributions, σ_z, of epoxy/Al composites with small particles of the second phase: (*a*) 12.5 vol pct of aluminum particles in the epoxy matrix (corresponds to mesh in Fig. 3(a)) and (*b*) 12.5 vol pct of epoxy particles in the aluminum matrix (corresponds to mesh in Fig. 3(c)).

oxy. This is due to the higher stiffness of aluminum. It should be noted that the mesh size corresponding to Figure 3(b) is not fine enough to comment about stress gradients. However, the mesh shown in Figure 4 is sufficient to show the stress gradient. Comparison of maximum and minimum stresses in Figures 10(a) and (b) shows that hydrostatic stress gradients increase with an increase in particle size. Further, Figure 10(b) also shows high hydrostatic stresses inside the alumina phase, at the interphase interfaces, which are approximately parallel to the loading direction, and the regions where the coarse particles come together. These are the preferred sites for initiation of voids or cracks. In addition, from Figures 10(a) and (b), it can be concluded that the propensity for formation of voids or cracks increases with an increase in particle size.

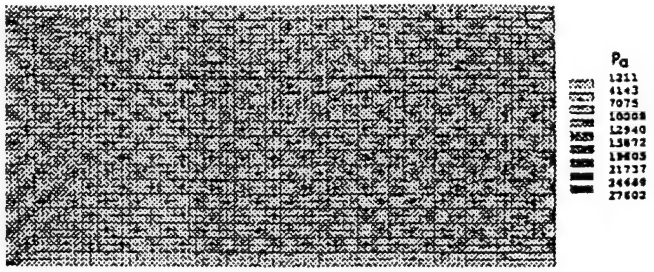

(*a*)

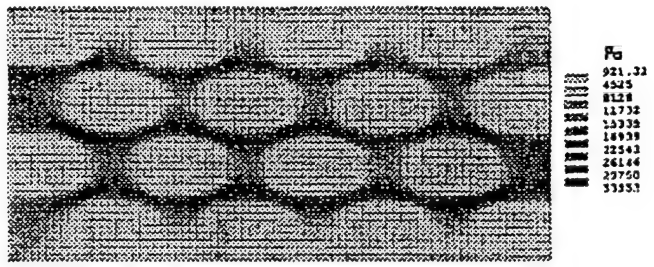

(*b*)

Fig. 10—The effect of particle size on the hydrostatic stress distribution, $(\sigma_x + \sigma_y)/2$, of epoxy/Al composite with 50 vol pct of each phase: (*a*) small-sized particle, four elements per particle, corresponds to Fig. 3(b); and (*b*) medium-sized particle, 81 elements per particle, corresponds to Fig. 4.

V. CONCLUSIONS

1. The loss factors of the composites with parallel and perpendicular fibers calculated by FEM were found to be close to those obtained by analytical methods based on the constant strain and constant stress assumptions.
2. For a given volume percent of Al or epoxy, the loss factor increased with an increase in relative particle size. This is attributed to the ability of the high damping epoxy phase to damp/deform relatively freely when the particle size is increased.
3. A 3-D plot with loss factor, relative particle size, and volume percent of Al as the parameters was constructed for the epoxy/Al composites, which clearly demonstrates the effect of particle size and volume percent of phases on the damping behavior.
4. For a composite with 50 vol pct of each phase, the loss factor of the composite when the Al phase was embedded as a single particle in the epoxy matrix was found to be much higher than when the phases were reversed. This is attributed to the ability of the epoxy to damp/deform relatively independently when it is the matrix phase.
5. For various epoxy/Al composites, normal stress distributions were also studied. They show that in general, the stresses are higher in the stiffer aluminum phase whether aluminum is in the form of particles or matrix. The extent of stress gradients depended on the volume fraction and particle size.
6. Two-dimensional hydrostatic stress distributions were also calculated for various epoxy/Al composites. It was found that the magnitude of stress gradients increases

with an increase in particle size for a given volume percent of phases. These results suggest that the propensity for void or crack formation increases with an increase in particle size.

ACKNOWLEDGMENTS

This work was funded by the Carderock Division of The Naval Surface Warfare Center and The Office Of Naval Research under Grant No. N00014-92-J-4039. The authors would like to express their appreciation to Mr. I.L. Caplan, Mrs. C.R. Wong, and Dr. L. Kabacoff for their interest and support.

REFERENCES

1. Z. Hashin: *Int. J. Solid Struct.*, 1970, vol. 6 (5), pp. 539-52.
2. Z. Hashin: *Int. J. Solid Struct.*, 1970, vol. 6 (6), pp. 797-807.
3. K.S. Kannan and S. Ankem: *Proc. Damping of Multiphase Inorganic Materials Symp.*, ASM Material Week, Chicago, IL, November 2–5, 1992, ASM INTERNATIONAL, Materials Park, OH, 1992, pp. 73-83.
4. C.P. Chen and R.S. Lakes: *J. Mater. Sci.*, 1993, vol. 28, pp. 4299-4304.
5. S.R. Ahmed and F.R. Jones: *J. Mater. Sci.*, 1990, vol. 25, pp. 4933-42.
6. S.N. Neti, A. Nanavaty, S. Ankem, and C.R. Wong: *M²D: Mechanics and Mechanisms of Material Damping*, ASTM STP 1169, ASTM, Philadelphia, PA, 1992, pp. 502-09.
7. *ANSYS Users Manual Ver. 4.4A*, Swanson Analysis System Inc., Houston, PA, 1972.
8. G.G. Wren and V.K. Kinra: *J. Test. Eval.*, 1988, vol. 16 (1), pp. 77-85.
9. R.M. Crane and J.W. Gillespie, Jr.: *Comp. Sci. Technol.*, 1991, vol. 40, pp. 355-75.
10. J. Zhang, R.J. Perez, and E.J. Lavernia: *J. Mater. Sci.*, 1993, vol. 28, pp. 2395-2404.
11. P.K. Rohatgi, N. Murali, H.R. Shetty, and R. Chandrasekhar: *Proc. Damping of Multiphase Inorganic Materials Symp.*, ASM Material Week, Chicago, IL, November 2–5, 1992, ASM INTERNATIONAL, Materials Park, OH, 1992, pp 103-13.
12. R.D. Adams and M.A.O. Fox: *J. Iron Steel Inst.*, 1973, vol. 211, pp. 37-43.

3. TECHNICAL PRESENTATIONS AND PUBLICATIONS

Presentations

1. 1992 TMS Fall Meeting, 2-5 November, 1992, "Recent Developments in Modeling the damping behavior of composites", K.S.Kannan and S.Ankem.

2. International Conference on "Advanced Composites 93", Wollongong, Australia, Feb. 1993, "The Effect of Morphology and Volume Fraction on the damping of Epoxy/Aluminium Composites", A.Nanavaty and S.Ankem.

3.1993 TMS Fall Meeting, Oct. 93, An International Symposium on M3D II: Mechanics and Mechanisms of Material Damping Behavior II, "The Effect of Volume Fraction and Morphology of Phases on the Damping Behavior of Epoxy-Aluminium Composites", J.G.Rao and S.Ankem.

Publications

1. "Recent Developments in Modeling the Damping Behavior of Composites", K.S.Kannan and S.Ankem, Proceedings of the Damping of Multiphase Inorganic Materials Symposium, ASM Material week Chicago, Nov. 1992, Ed. R.B. Bhagat, ASM International, 1993, pp. 73-83.

2. "The effect of Morphology and Volume Fraction on the Damping of Epoxy/Aluminium Composites", A.Nanavaty and S.Ankem, Proceedings of the International Conference on Advanced Composite Materials, Advanced Composites '93, Eds. T.Chandra and A.K.Dingra, TMS, 1993, pp. 1325-1328.

3. "The Effect of Volume Percent and Morphology of Phases on the Damping Behavior of Epoxy/Aluminium Composites", J.G.Rao and S.Ankem, Accepted for publication in Metallurgical and Materials Transactions A, 1995.

4. APPENDIX : SAMPLE INPUT AND OUTPUT FOR A 50 VOLUME PERCENT Al - EPOXY COMPOSITE

```
/batch

/prep7
/show,x11-gray
/TITLE, EPOXY-AL, 50 VOL.%  PARALLEL FIBERS - ETA


k,1,0,0,0
k,2,0.1905,0,0
kgen,13,1,2,,0,0.00733,,2
kplot
l,1,2
lgen,13,1,,,,0.00733,,2
lplot
ldvs,all,,24,1,1
l,1,3
lgen,12,14,,,,0.00733,,2
lplot
l,2,4
lgen,12,26,,,,0.00733,,2
ldvs,all,,1,1,0
lplot
A,1,2,4,3
AGEN,12,1,,,,0.00733,,2
APLOT
!! APPLYING THE MATERIAL PROPERTIES

KAN,6

ET,1,42,0,1,3,,0,0,0
MP,EX,1,6.9E10
MP,EY,1,6.9E10
,NUXY,1,0.34
,DENS,1,2700
,DAMP,1,0.0159E-02
,EX,2,6.9E09
,EY,2,6.9E09
,NUXY,2,0.34-
,DENS,2,1194.2
,DAMP,2,0.0159
R,1,0.0203
AATT,1,1,1,0
AMESH,1,11,2
AATT,2,1,1,0
AMESH,2,12,2
WAVES
/PNUM,KPOI,0
/PNUM,ELEM,0
/PNUM,NODE,1


!CPSIZE,25
CP,1,UX,2,26,52,76,102,126,152,176,202
CP,1,UX,226,252,276,301

FINISH
!
! APPLY LOADS AND OBTAIN THE SOLUTION


/SOLU

ANTYPE,HARMIC            !HARMONIC ANALYSIS
HROPT,FULL               !FULL METHOD
HROUT,OFF
```

```
D,1,ALL,0,,251,50
D,27,ALL,0,,277,50
D,302,ALL,0

M,2,UX
TOTAL,50
F,2,FX,40.08


ITER,2,1
HARFRQ,0,2
KAY,3,1
KBC,1
SAVE

/PBC,ALL,1
/PNUM,ELEM,0
/PNUM,KPOI,0
/SHOW,PLOTS1,GRPH
/PNUM,MAT,1
/NUMBER,1

SAVE
/output,prob50,out
/nerr
SOLVE
FINISH

/STRESS
ITER,2,1
HARFRQ,0,2
NSTRESS,1
END
FINISH


!
! REVIEW THE RESULTS
/POST1
SET,1,1
/PNUM,MAT,1
/NUMBER,0
PLNSTR,SX
PLDISP,1
FINISH
```

NUMBER OF DISPLAYED ERRORS ALLOWED PER COMMAND= 200
NUMBER OF ERRORS ALLOWED PER COMMAND BEFORE ANSYS ABORT= 10000

***** ANSYS SOLVE COMMAND *****

*** NOTE *** CP= 11.320 TIME= 15:03:36
All shape tests were bypassed for elements associated with the solid model, because most of them were already done at AMESH or VMESH. Use CHECK if desired to perform all of the element tests.
1

***** ANSYS - ENGINEERING ANALYSIS SYSTEM REVISION 5.0 24 *****
UNIV. MARYLAND VERSION=SUN4SPARC 15:03:36 MAR 15, 1995 CP= 11.330
FOR SUPPORT CALL DOUG MOHNEY PHONE (301) 405-5317 FAX

EPOXY-AL, 50 VOL.% PARALLEL FIBERS - ETA

ANSYS VERSION FOR EDUCATIONAL PURPOSES ONLY

S O L U T I O N O P T I O N S

PROBLEM DIMENSIONALITY. 2-D
DEGREES OF FREEDOM. . . . . UX UY
ANALYSIS TYPE . . . . . .HARMONIC
SOLUTION METHOD. . . . . .FULL
COMPLEX DISPLACEMENT PRINT OPTION . . . . . .AMPLITUDE AND PHASE ANGLE

L O A D S T E P O P T I O N S

LOAD STEP NUMBER. 1
FREQUENCY RANGE . . . . . 0. TO 2.0000
NUMBER OF SUBSTEPS. 2
STEP CHANGE BOUNDARY CONDITIONS . . . . . YES
PRINT OUTPUT CONTROLS
ITEM FREQUENCY COMPONENT
BASI ALL
DATABASE OUTPUT CONTROLS
ITEM FREQUENCY COMPONENT
ALL LAST

***** CENTROID, MASS, AND MASS MOMENTS OF INERTIA *****

CALCULATIONS ASSUME ELEMENT MASS AT ELEMENT CENTROID

TOTAL MASS = 0.66231

CENTROID		MOM. OF INERTIA ABOUT ORIGIN		MOM. OF INERTIA ABOUT CENTROID	
XC =	0.95250E-01	IXX =	0.1623E-02	IXX =	0.4227E-03
YC =	0.42563E-01	IYY =	0.8008E-02	IYY =	0.1999E-02
ZC =	0.	IZZ =	0.9631E-02	IZZ =	0.2422E-02
		IXY =	-0.2685E-02	IXY =	-0.4770E-17
		IYZ =	0.	IYZ =	0.
		IZX =	0.	IZX =	0.

*** MASS SUMMARY BY ELEMENT TYPE ***

TYPE	MASS
1	0.662315

Range of element maximum matrix coefficients in global coordinates
Maximum= 732565196. at element 144.
Minimum= 73256519.6 at element 284.

*** ELEMENT MATRIX FORMULATION TIMES

TYPE	NUMBER	ENAME	TOTAL CP	AVE CP
1	288	PLANE42	1.850	0.006

Time at end of element matrix formulation CP= 13.6499997.

Estimated number of active DOF= 612.
Maximum wavefront= 38.

Time at end of matrix triangularization CP= 15.5099994.
Equation solver maximum pivot= 9.129143316E+09 at node 2 UX.
Equation solver minimum pivot= 68660137.7 at node 301 UY.
1

***** ANSYS - ENGINEERING ANALYSIS SYSTEM REVISION 5.0 24 *****
UNIV. MARYLAND VERSION=SUN4SPARC 15:03:48 MAR 15, 1995 CP= 15.660
FOR SUPPORT CALL DOUG MOHNEY PHONE (301) 405-5317 FAX

EPOXY-AL, 50 VOL.% PARALLEL FIBERS - ETA

ANSYS VERSION FOR EDUCATIONAL PURPOSES ONLY

***** COMPLEX DEGREE OF FREEDOM SOLUTION ***** FREQUENCY = 1.0000
LOAD STEP= 1 SUBSTEP = 1 CUM. ITER.= 1

***** AMPLITUDE AND PHASE ANGLE (DEGREES) *****

	UX		UY	
1	0.	0.	0.	0.
2	0.112179E-06	-0.581567	0.836666E-08	-0.469408
3	0.547407E-08	-0.313518	0.275602E-08	0.793089
4	0.102441E-07	-0.505779	0.477911E-08	0.486703
5	0.146852E-07	-0.570727	0.638244E-08	0.865926E-01
6	0.191211E-07	-0.587649	0.734330E-08	-0.180039
7	0.236076E-07	-0.591640	0.788894E-08	-0.334874
8	0.281479E-07	-0.593419	0.817936E-08	-0.413716
9	0.327291E-07	-0.594809	0.832561E-08	-0.449175
10	0.373399E-07	-0.595646	0.839248E-08	-0.462939
11	0.419721E-07	-0.595780	0.841734E-08	-0.467112
12	0.466199E-07	-0.595295	0.842131E-08	-0.467683
13	0.512791E-07	-0.594374	0.841600E-08	-0.467327
14	0.559466E-07	-0.593195	0.840753E-08	-0.467069
15	0.606202E-07	-0.591896	0.839881E-08	-0.467160
16	0.652984E-07	-0.590575	0.839108E-08	-0.467536
17	0.699799E-07	-0.589292	0.838471E-08	-0.468042
18	0.746640E-07	-0.588085	0.837967E-08	-0.468541
19	0.793501E-07	-0.586970	0.837579E-08	-0.468947
20	0.840377E-07	-0.585952	0.837285E-08	-0.469228
21	0.887264E-07	-0.585029	0.837067E-08	-0.469389
22	0.934160E-07	-0.584195	0.836908E-08	-0.469457
23	0.981062E-07	-0.583441	0.836796E-08	-0.469463
24	0.102797E-06	-0.582757	0.836722E-08	-0.469442
25	0.107488E-06	-0.582136	0.836680E-08	-0.469418
26	0.112179E-06	-0.581567	0.689374E-08	-0.448225
27	0.	0.	0.	0.
28	0.381279E-08	-0.560028	0.108769E-08	3.18870
29	0.863000E-08	-0.466690	0.337992E-08	0.950052
30	0.135666E-07	-0.487771	0.491897E-08	0.300277
31	0.184419E-07	-0.530275	0.588982E-08	-0.659664E-01
32	0.232230E-07	-0.562596	0.643479E-08	-0.265082

33	0.279396E-07	-0.581674	0.672530E-08	-0.366087
34	0.326212E-07	-0.591252	0.686975E-08	-0.412998
35	0.372877E-07	-0.595277	0.693414E-08	-0.432765
36	0.419497E-07	-0.596358	0.695641E-08	-0.440159
37	0.466127E-07	-0.595967	0.695800E-08	-0.442563
38	0.512790E-07	-0.594881	0.695066E-08	-0.443360
39	0.559494E-07	-0.593509	0.694049E-08	-0.443913
40	0.606237E-07	-0.592061	0.693041E-08	-0.444622
41	0.653016E-07	-0.590644	0.692159E-08	-0.445477
42	0.699826E-07	-0.589310	0.691436E-08	-0.446345
43	0.746661E-07	-0.588080	0.690864E-08	-0.447102
44	0.793517E-07	-0.586957	0.690422E-08	-0.447677
45	0.840388E-07	-0.585941	0.690087E-08	-0.448053
46	0.887272E-07	-0.585021	0.689837E-08	-0.448256
47	0.934166E-07	-0.584191	0.689654E-08	-0.448328
48	0.981066E-07	-0.583439	0.689524E-08	-0.448321
49	0.102797E-06	-0.582757	0.689439E-08	-0.448280
50	0.107488E-06	-0.582136	0.689390E-08	-0.448241
51	0.	0.	0.	0.
52	0.112179E-06	-0.581567	0.541935E-08	-0.413690
53	0.469594E-08	-0.663400	0.160672E-08	0.239459
54	0.931184E-08	-0.704802	0.270546E-08	0.425068
55	0.138627E-07	-0.676015	0.379201E-08	0.183320
56	0.184402E-07	-0.646782	0.453923E-08	-0.360391E-01
57	0.230522E-07	-0.624986	0.500664E-08	-0.199671
58	0.276981E-07	-0.610716	0.526648E-08	-0.302816
59	0.323686E-07	-0.602018	0.539737E-08	-0.359193
60	0.370542E-07	-0.596882	0.545513E-08	-0.386076
61	0.417476E-07	-0.593785	0.547474E-08	-0.397471
62	0.464443E-07	-0.591769	0.547602E-08	-0.402119
63	0.511419E-07	-0.590306	0.546954E-08	-0.404423
64	0.558394E-07	-0.589132	0.546064E-08	-0.406158
65	0.605363E-07	-0.588123	0.545181E-08	-0.407823
66	0.652326E-07	-0.587224	0.544407E-08	-0.409423
67	0.699283E-07	-0.586409	0.543769E-08	-0.410843
68	0.746236E-07	-0.585665	0.543262E-08	-0.411988
69	0.793185E-07	-0.584984	0.542870E-08	-0.412822
70	0.840132E-07	-0.584360	0.542572E-08	-0.413360
71	0.887077E-07	-0.583789	0.542349E-08	-0.413655
72	0.934021E-07	-0.583265	0.542185E-08	-0.413774
73	0.980964E-07	-0.582785	0.542070E-08	-0.413786
74	0.102791E-06	-0.582344	0.541993E-08	-0.413748
75	0.107485E-06	-0.581939	0.541949E-08	-0.413707
76	0.112179E-06	-0.581567	0.394526E-08	-0.354136
77	0.	0.	0.	0.
78	0.394759E-08	-0.736900	0.166556E-09	14.9872
79	0.847414E-08	-0.673200	0.142433E-08	1.65411
80	0.131680E-07	-0.633260	0.238476E-08	0.707572
81	0.179496E-07	-0.614791	0.309802E-08	0.230489
82	0.227421E-07	-0.606684	0.354179E-08	-0.427582E-01
83	0.275173E-07	-0.602770	0.379215E-08	-0.198871
84	0.322693E-07	-0.600021	0.391907E-08	-0.280732
85	0.370020E-07	-0.597511	0.397576E-08	-0.319026
86	0.417211E-07	-0.595166	0.399556E-08	-0.334916
87	0.464313E-07	-0.593080	0.399755E-08	-0.341039
88	0.511357E-07	-0.591301	0.399193E-08	-0.343746
89	0.558365E-07	-0.589807	0.398383E-08	-0.345637
90	0.605349E-07	-0.588552	0.397569E-08	-0.347477
91	0.652318E-07	-0.587484	0.396849E-08	-0.349303
92	0.699278E-07	-0.586561	0.396253E-08	-0.350958
93	0.746231E-07	-0.585752	0.395778E-08	-0.352306
94	0.793181E-07	-0.585034	0.395410E-08	-0.353284
95	0.840128E-07	-0.584389	0.395128E-08	-0.353904
96	0.887073E-07	-0.583806	0.394918E-08	-0.354225
97	0.934017E-07	-0.583276	0.394763E-08	-0.354331
98	0.980961E-07	-0.582792	0.394654E-08	-0.354308

33	0.279396E-07	-0.581674	0.672530E-08	-0.366087
34	0.326212E-07	-0.591252	0.686975E-08	-0.412998
35	0.372877E-07	-0.595277	0.693414E-08	-0.432765
36	0.419497E-07	-0.596358	0.695641E-08	-0.440159
37	0.466127E-07	-0.595967	0.695800E-08	-0.442563
38	0.512790E-07	-0.594881	0.695066E-08	-0.443360
39	0.559494E-07	-0.593509	0.694049E-08	-0.443913
40	0.606237E-07	-0.592061	0.693041E-08	-0.444622
41	0.653016E-07	-0.590644	0.692159E-08	-0.445477
42	0.699826E-07	-0.589310	0.691436E-08	-0.446345
43	0.746661E-07	-0.588080	0.690864E-08	-0.447102
44	0.793517E-07	-0.586957	0.690422E-08	-0.447677
45	0.840388E-07	-0.585941	0.690087E-08	-0.448053
46	0.887272E-07	-0.585021	0.689837E-08	-0.448256
47	0.934166E-07	-0.584191	0.689654E-08	-0.448328
48	0.981066E-07	-0.583439	0.689524E-08	-0.448321
49	0.102797E-06	-0.582757	0.689439E-08	-0.448280
50	0.107488E-06	-0.582136	0.689390E-08	-0.448241
51	0.	0.	0.	0.
52	0.112179E-06	-0.581567	0.541935E-08	-0.413690
53	0.469594E-08	-0.663400	0.160672E-08	0.239459
54	0.931184E-08	-0.704802	0.270546E-08	0.425068
55	0.138627E-07	-0.676015	0.379201E-08	0.183320
56	0.184402E-07	-0.646782	0.453923E-08	-0.360391E-01
57	0.230522E-07	-0.624986	0.500664E-08	-0.199671
58	0.276981E-07	-0.610716	0.526648E-08	-0.302816
59	0.323686E-07	-0.602018	0.539737E-08	-0.359193
60	0.370542E-07	-0.596882	0.545513E-08	-0.386076
61	0.417476E-07	-0.593785	0.547474E-08	-0.397471
62	0.464443E-07	-0.591769	0.547602E-08	-0.402119
63	0.511419E-07	-0.590306	0.546954E-08	-0.404423
64	0.558394E-07	-0.589132	0.546064E-08	-0.406158
65	0.605363E-07	-0.588123	0.545181E-08	-0.407823
66	0.652326E-07	-0.587224	0.544407E-08	-0.409423
67	0.699283E-07	-0.586409	0.543769E-08	-0.410843
68	0.746236E-07	-0.585665	0.543262E-08	-0.411988
69	0.793185E-07	-0.584984	0.542870E-08	-0.412822
70	0.840132E-07	-0.584360	0.542572E-08	-0.413360
71	0.887077E-07	-0.583789	0.542349E-08	-0.413655
72	0.934021E-07	-0.583265	0.542185E-08	-0.413774
73	0.980964E-07	-0.582785	0.542070E-08	-0.413786
74	0.102791E-06	-0.582344	0.541993E-08	-0.413748
75	0.107485E-06	-0.581939	0.541949E-08	-0.413707
76	0.112179E-06	-0.581567	0.394526E-08	-0.354136
77	0.	0.	0.	0.
78	0.394759E-08	-0.736900	0.166556E-09	14.9872
79	0.847414E-08	-0.673200	0.142433E-08	1.65411
80	0.131680E-07	-0.633260	0.238476E-08	0.707572
81	0.179496E-07	-0.614791	0.309802E-08	0.230489
82	0.227421E-07	-0.606684	0.354179E-08	-0.427582E-01
83	0.275173E-07	-0.602770	0.379215E-08	-0.198871
84	0.322693E-07	-0.600021	0.391907E-08	-0.280732
85	0.370020E-07	-0.597511	0.397576E-08	-0.319026
86	0.417211E-07	-0.595166	0.399556E-08	-0.334916
87	0.464313E-07	-0.593080	0.399755E-08	-0.341039
88	0.511357E-07	-0.591301	0.399193E-08	-0.343746
89	0.558365E-07	-0.589807	0.398383E-08	-0.345637
90	0.605349E-07	-0.588552	0.397569E-08	-0.347477
91	0.652318E-07	-0.587484	0.396849E-08	-0.349303
92	0.699278E-07	-0.586561	0.396253E-08	-0.350958
93	0.746231E-07	-0.585752	0.395778E-08	-0.352306
94	0.793181E-07	-0.585034	0.395410E-08	-0.353284
95	0.840128E-07	-0.584389	0.395128E-08	-0.353904
96	0.887073E-07	-0.583806	0.394918E-08	-0.354225
97	0.934017E-07	-0.583276	0.394763E-08	-0.354331
98	0.980961E-07	-0.582792	0.394654E-08	-0.354308